

AD-A090 610 CALIFORNIA UNIV LOS ANGELES PLASMA PHYSICS GROUP F/G 20/9
EFFECT OF A DC ELECTRIC FIELD ON THE TRAPPING DYNAMICS OF A COL--ETC(U)
OCT 79 G J MORALES N00014-75-C-0476
UNCLASSIFIED PPG-439 NL

CALIFORNIA UNIV LOS ANGELES PLASMA PHYSICS GROUP F/G 20/9
EFFECT OF A DC ELECTRIC FIELD ON THE TRAPPING DYNAMICS OF A COL--ETC(U)
OCT 79 G J MORALES N00014-75-C-0476
PPG-439 NL

UNCLASSIFIED

PPG-439

NL

END

DATE _____

FILMED

11-13

DTIC

AD A090810

DDC FILE COPY

U.S. DEPARTMENT OF ENERGY

LEVEL II

①

CENTER FOR
PLASMA PHYSICS
AND
FUSION ENGINEERING
UNIVERSITY OF CALIFORNIA
LOS ANGELES

DTIC
ELECTE
SEP 30 1980
A

DISTRIBUTION STATEMENT A

Approved for public release;
Distribution Unlimited

80 9 15 126

SECURITY CLASSIFICATION OF THIS PAGE (When Data Entered)

REPORT DOCUMENTATION PAGE		READ INSTRUCTIONS BEFORE COMPLETING FORM
1. REPORT NUMBER PPG-439 ✓	2. GOVT ACCESSION NO. AD-A090	3. RECIPIENT'S CATALOG NUMBER 810
4. TITLE (and Subtitle) ^{DC} EFFECT OF A VS ELECTRIC FIELD ON THE TRAPPING DYNAMICS OF A COLD ELECTRON BEAM		5. TYPE OF REPORT & PERIOD COVERED
		6. PERFORMING ORG. REPORT NUMBER
7. AUTHOR(s) G. J. Morales		8. CONTRACT OR GRANT NUMBER(s) N00014-75-C-0476 ✓
9. PERFORMING ORGANIZATION NAME AND ADDRESS University of California 405 Hilgard Avenue, Knudsen 1-130 Los Angeles, CA 90024		10. PROGRAM ELEMENT, PROJECT, TASK AREA & WORK UNIT NUMBERS
11. CONTROLLING OFFICE NAME AND ADDRESS		12. REPORT DATE October, 1979
		13. NUMBER OF PAGES 64
14. MONITORING AGENCY NAME & ADDRESS (if different from Controlling Office)		15. SECURITY CLASS. (of this report)
		15a. DECLASSIFICATION/DOWNGRADING SCHEDULE
16. DISTRIBUTION STATEMENT (of this Report)		
17. DISTRIBUTION STATEMENT (of the abstract entered in Block 20, if different from Report)		
18. SUPPLEMENTARY NOTES		
19. KEY WORDS (Continue on reverse side if necessary and identify by block number) Self consistent modification of the trapping dynamics of a low density cold electron beam due to the external application of a DC electric field.		
20. ABSTRACT (Continue on reverse side if necessary and identify by block number) on back page.		

DD FORM 1 JAN 73 1473

EDITION OF 1 NOV 68 IS OBSOLETE
S/N 0102-LF-014-6601

SECURITY CLASSIFICATION OF THIS PAGE (When Data Entered)

ABSTRACT

↙ This study considers the self-consistent modification of the trapping dynamics of a low density cold electron beam due to the external application of a DC electric field. For DC fields smaller than the peak amplitude of the saturated beam-plasma instability, the beam energy remains clamped while the wave amplitude grows secularly. Large travelling potential wells appear and create strongly focused charge clumps. By considering the role of wave dissipation an exact dynamic BGL (Bernstein-Green-Kruskal) equilibrium is found analytically. It consists of a singular charge clump which propagates through the medium at constant velocity even though a DC field is present. The numerical study of the basic equations shows that the system evolves asymptotically to this singular state. A variety of experimentally relevant phenomena associated with the trapping dynamics is investigated, including the stability of the dynamic nonlinear equilibrium to sideband growth.

↙

LEVEL II

①

⑥
EFFECT OF A DC ELECTRIC FIELD ON THE
TRAPPING DYNAMICS OF A COLD ELECTRON BEAM

⑩
G. J. Morales

⑭
PPG-439

⑪
October 1979

⑫ 67

⑮
Contract N00014-75-C-0476

DTIC
ELECTE
SEP 30 1980

A

Physics Department
University of California, Los Angeles
Los Angeles, California 90024

DISTRIBUTION STATEMENT A
Approved for public release;
Distribution Unlimited

JB

401733

ABSTRACT

This study considers the self-consistent modification of the trapping dynamics of a low density cold electron beam due to the external application of a DC electric field. For DC fields smaller than the peak amplitude of the saturated beam-plasma instability, the beam energy remains clamped while the wave amplitude grows secularly. Large travelling potential wells appear and create strongly focused charge clumps. By considering the role of wave dissipation an exact dynamic BGK (Bernstein-Greene-Kruskal) equilibrium is found analytically. It consists of a singular charge clump which propagates through the medium at constant velocity even though a DC field is present. The numerical study of the basic equations shows that the system evolves asymptotically to this singular state. A variety of experimentally relevant phenomena associated with the trapping dynamics is investigated, including the stability of the dynamic nonlinear equilibrium to sideband growth.

Accession For	
NTIS GRA&I	<input checked="checked" type="checkbox"/>
DDC TAB	<input type="checkbox"/>
Unannounced	<input type="checkbox"/>
Justification <i>for</i>	
<i>Letter on File</i>	
By _____	
Distribution/	
Availability Codes	
Dist.	Avail and/or special
<i>A</i>	

I. Introduction

The trapping of charged particles within the travelling potential wells of collective plasma oscillations is one of the more significant strong nonlinearities encountered in plasmas. Particle trapping is known, both theoretically^{1,2} and experimentally³, to alter the linear collisionless damping (Landau damping) of collective modes supported by plasmas, and it is one of the dominant mechanisms that limits the growth of velocity-space instabilities. The strong effects produced by particle trapping are related to the formation of phase-space granulations out of initially smooth contours. The phase-space granulation is partially reversible, and under carefully selected conditions can lead to interesting amplitude^{4,5} and phase^{5,6} oscillations which persist for relative long times of experimental interest. The phase-space granulation can disappear smoothly by the process of phase mixing while the charged particles remain confined within the potential wells, as is characteristic of the time asymptotic formation of steady Bernstein-Greene-Kruskal⁷ (BKG) modes. The granulation can also disappear more abruptly if the trapped particles escape from the potential wells, as may occur due to the spontaneous growth of sideband waves, sudden phase slippage due to finite dissipation⁸, or the launching of other large amplitude waves.⁹

The present study is concerned with the dynamics of trapped particles and the associated phase-space granulation in the presence of an externally applied DC electric field. The motivation for investigating this dynamical system in detail can be attributed to the finding in a previous theoretical study¹⁰ that the momentum of a runaway beam can become clamped due to the excitation of modes travelling in synchronism with the beam. That earlier study was in turn stimulated by the experimental observation^{11,12} of runaway energy clamping in the Microtor Tokamak at the University of California, Los Angeles.

As is expected, the beam clamping effect sets in when the amplitude of the resonant wave becomes larger than the external DC electric field. The earlier calculation of this effect has been accomplished by means of a spatially averaged formalism based on the exact conservation laws for energy and momentum, but with the restrictive implicit assumption that the phase-space granulation is instantaneously smeared out, i.e., the runaway beam acquires an irreversible thermal spread. Of course, in reality the trapped particle dynamics is partially reversible. Therefore, it is of interest to elucidate the underlying single particle dynamics accompanying the clamping process, to validate the existence of clamping independently of the spatially averaged formalism, and to establish the limitations of the latter. In addition, there are various associated effects which are of interest for both basic and applied reasons. A preliminary study of some of these effects has been previously discussed^{13,14} by this author.

To isolate the principal effects produced by an external DC electric field E_0 , we consider the cleanest environment for trapped particle dynamics, i.e., the low density cold beam problem in which the background component supporting the waves remains strictly linear. In practice this situation can be realized by having a cold background plasma with heavy ions or simply replacing the cold plasma by a slow wave structure, as is commonly done in travelling wave tube (TWT) devices.⁸ The cold plasma assumption can be met by supplying sufficient neutral gas in order to compensate for the heating produced by the waves and the intrinsic ohmic heating associated with E_0 .

It is well known^{8,15-17} that in the absence of the DC electric field the weak cold beam amplifies a narrow spectrum of noise waves supported by the background structure. After several e-foldings the noise evolves into a nearly monochromatic signal (single mode) whose growth is stopped by the abrupt trapping

of the beam electrons within its potential troughs. The application of a DC electric field to this system is found to produce a secular growth in the wave amplitude without a noticeable increase in the beam momentum, i.e., the external momentum push is transferred to the wave while the beam remains clamped. This result is obtained in the present study by following the self-consistent orbits of the trapped particles in a digital computer, thus confirming the existence of beam clamping predicted by the earlier spatially averaged analysis.¹⁰ However, additional features associated with the trapping dynamics are uncovered. One of them is the expected appearance of trapping oscillations of increasing frequency which modulate the secular growth in the wave amplitude. Another feature is the generation of secondary low density runaway beams which arise from the spillage of the primary beam particles out of the potential wells.

In the absence of wave damping the secular increase in the wave amplitude produced by the DC electric field is unbounded. Large potential wells are generated and the trapped particles evolve into phase-space clumps of ever decreasing dimensions. When a wave dissipation channel exists, one obtains analytically an exact dynamic BGK equilibrium consisting of a singular charge clump which is being pushed by E_0 , but whose momentum remains constant. This unusual and highly nonlinear state is found to be approached asymptotically by the time dependent computer solution of the problem.

The application of the DC electric field permits the detailed manipulation of the position of the trapped particles relative to the bottom of the potential wells of the wave. By changing the direction of the DC field, one can either make the wave grow or damp. By means of this phase-space reconstruction, it is possible to reverse the drastic disappearance of the trapped particle oscillations associated with finite wave dissipation.

The enhanced growth in the wave amplitude produced by E_0 can be used to improve the efficiency of a TWT, as was investigated nearly twenty years ago by Hess.¹⁸ A similar application may be found for the collective free electron lasers under present consideration¹⁹, where particle trapping plays an important role. The results presented here illuminate some of the fundamental processes which underly these practical developments, and define specific experiments amenable to investigation in the laboratory.

In Section II of the paper some of the basic properties of trapping behavior in the presence of a DC electric field are examined analytically. The weak cold beam formalism is examined in Section III. The beam clamping effect is discussed in Section IV, and the dynamic BGK equilibrium is explained in Section V. The stability of the singular clump equilibrium to sideband growth is investigated in Section VI. Concluding remarks are presented in Section VII.

II. Modified Trapping Behavior

Before considering the self-consistent evolution of the wave amplitude and phase together with the trapped particle dynamics in the presence of an external DC electric field, it is useful to develop a simple description of the lowest order effects produced by the DC field on particles which are trapped in an electrostatic wave of fixed amplitude and phase velocity. In this case, the equation of motion for electrons of charge $-e$, and mass m , in the wave frame moving with speed ω/k relative to the laboratory is

$$m \frac{d^2}{dt^2} x = -eA \sin(kx) + eE_0 \quad (1)$$

where A is the wave amplitude, k the wavenumber, and ω the frequency.

It is evident from Eq (1) that the particles move in a distorted potential well whose potential energy function U is

$$U = -(eA/k) \left[(kxE_0/A) + \cos(kx) \right] \quad (2)$$

The spatial behavior of the corresponding potential well is exhibited in Fig. 1 for the values $E_0/A = 0.2, 0.5, 0.9$, over the interval $-\pi \leq kx \leq \pi$. It is seen that particle trapping ceases to exist when $E_0 \geq A$, since only a single turning point is found for the potential. This trapping threshold is a useful comparison standard for the studies of Sec III, where it is shown that this threshold can be exceeded by a factor of 2 when the self-consistent amplitude and phase changes are considered.

For $E_0 \neq 0$, the bottom of the potential well is shifted from $x = 0$ to a location x_s given by

$$X_s = R^{-1} \Delta M^{-1} (E_0/A) \quad (3)$$

and the corresponding bounce time t_b is

$$t_b = (2/\omega_b) \int_{\xi_1}^{\xi_2} \frac{d\xi}{\left[U_0 + 2[\cos \xi + (\xi E_0/A)] \right]^{1/2}} \quad (4)$$

instead of the usual elliptic integral expression. In Eq (4), $\omega_b = (eAk/m)^{1/2}$ is the bounce frequency for $E_0=0$, $U_0 = U(t=0)/(eA/k)$ is the scaled energy of the particle, $\xi = kx$, and ξ_1, ξ_2 refer to the turning points, which are not symmetric.

The lowest order correction to the bounce frequency of particles bouncing near the bottom of the distorted well can be extracted through the Bogoliuvov procedure²⁰ applied to the equation

$$\frac{d^2}{d\tau^2} \xi = -\sin(\eta + \xi_s) + E_0/A \quad (5)$$

where $\xi_s = kx_s$, $\xi = \eta + \xi_s$, and $\tau = \omega_b t$. For small displacements $|\eta| \ll 1$, Eq (1) can be approximated by

$$\frac{d^2}{d\tau^2} \eta + (\cos \xi_s) \eta \approx (E_0/2A) \eta^2 + (E_0/A)^3 (\cos \xi_s)/6 \quad (6)$$

Taking the solution to be of the form

$$\eta(\tau) = a(\tau) \sin[\theta(\tau)] \quad (7)$$

and eliminating the secular behavior in lowest order leads to

$$\frac{d}{d\tau} a = a^2 (\xi_s E_0 / 2A) (2\pi \cos \xi_s)^{-1} \int_0^{2\pi} d\theta \cos \theta \sin^2 \theta$$

$$\frac{d}{d\tau} a = 0 \quad (8)$$

and

$$\frac{d}{d\tau} \theta = (\cos \xi_s)^{1/2} - (\cos \xi_s)^{1/2} (E_0 / A)^2 (18\pi a)^{-1} \int_0^{2\pi} d\theta \sin^4 \theta$$

$$\frac{d}{d\tau} \theta = (\cos \xi_s)^{1/2} (1 - a^2 / 16) \quad (9)$$

which results in the modified bounce frequency $\bar{\omega}_b$

$$\bar{\omega}_b = (e k A / m)^{1/2} [1 - (E_0 / A)^2]^{1/4} [1 - (k x_0 / 4)^2] \quad (10)$$

for a particle of initial displacement x_0 . It is seen explicitly from Eq (10) that the application of the DC electric field weakens the restoring force provided by the wave potential, and furthermore that bouncing ceases to exist as E_0 approaches A .

The distortion of the well produced by $E_0 \neq 0$ gives rise to the detrapping of some particles which for $E_0 = 0$ would remain confined within the wave troughs. The time evolution of the orbits of these detrapped particles can be obtained by solving Eq (1) in a perturbative manner, i.e., taking the lowest order orbit ξ_0 to be

$$\xi_0(\tau) = \xi(0) + \dot{\xi}(0)\tau + \lambda \tau^2 / 2$$

$$\lambda = E_0 / A \quad (11)$$

The scaled equation for the first order velocity becomes

$$\frac{d^2}{d\tau^2} \xi_1 \approx - \sin [\xi(0) + \dot{\xi}(0)\tau + \lambda\tau^2/2] \quad (12)$$

whose exact solution can be expressed in the terms of the Si (sine) and Ci (cosine) integrals, i.e.,

$$\dot{\xi}_1(\tau) = - (2\lambda)^{-1/2} \left\{ \begin{aligned} & \{Ci[z(\tau)] - Ci[z(0)]\} \sin \theta_0 \\ & + \{Si[z(\tau)] - Si[z(0)]\} \cos \theta_0 \end{aligned} \right\} \quad (13)$$

where,

$$\begin{aligned} \theta_0 &= \xi(0) - [\dot{\xi}(0)]^2/2\lambda \\ z(\tau) &= (\lambda/2)^{1/2} \tau + \dot{\xi}(0)/(2\lambda)^{1/2} \end{aligned} \quad (14)$$

The asymptotic behavior sets in²¹ for $z > 4$ and the leading expansions are

$$\begin{aligned} Si &\approx \pi/2 - \cos z/z \\ Ci &\approx \sin z/z \end{aligned} \quad (15)$$

thus indicating that the detrapped particles become runaways which exhibit decreasing oscillations with a frequency $\omega_R = \omega_b (E_0/2A)^{1/2} = (ekE_0/2m)^{1/2}$. The net effect of the wave potential on the runaway electrons created by the detrapping process is to modify the free-fall velocity by an amount δv given by

$$\Delta V = (\omega_b/k)(A/2E_0)^{1/2} \left\{ \sin \theta_0 [z(0)] - \cos \theta_0 [\pi/2 - \text{Si}[z(0)]] \right\} \quad (16)$$

over a characteristic time $\Delta t \sim 10/\omega_R$.

The displacement of the bottom of the effective potential given by Eq (3) plays a major role in the time evolution of the wave amplitude. Essentially, the forward push provided by E_0 overcomes the particle recoil associated with momentum transfer to the wave. Hence, a particle remains in synchronism with the wave and causes a secular increase in its amplitude, as is discussed in Sec III. Therefore, an additional consequence of $E_0 \neq 0$ is that the depth of the trapping well increases in time if E_0 is less than the threshold value for the destruction of trapping (i.e., $E_0 < A$ to lowest order). An exactly soluble simplified model of particle trapping in this environment is described by the equation

$$m \frac{d^2}{dt^2} x + e A (1 + \alpha t) (kx) = e E_0 \quad (17)$$

where α measures the rate of increase of the wave amplitude. Defining the auxiliary variables

$$\begin{aligned} \eta &= (\omega_b/\alpha)^{3/2} (1 + \alpha t) \\ \xi &= (\alpha/\omega_b)^{2/3} (A/E_0) (kx) \end{aligned} \quad (18)$$

transforms Eq (17) into

$$\frac{d^2}{d\eta^2} z + \eta z = 1 \quad (19)$$

which is the inhomogeneous Airy equation whose solution for a particle initially trapped at the bottom of the potential well (i.e., $z = dz/d\eta = 0$ at $t = 0$) is given by

$$z(\eta) = \pi^2 [a \text{Ai}(\eta) + b \text{Bi}(\eta) - \pi^{-1} \text{Gi}(\eta)] \quad (20)$$

where Ai, Bi, and Gi are the standard Airy functions. The constants a and b are

$$\begin{aligned} a &= (G_i' \text{Bi} - G_i \text{Bi}') / \text{Bi}' \\ b &= (G_i' \text{Ai} - G_i \text{Ai}') / \text{Ai}' \end{aligned} \quad (21)$$

where the prime denotes a derivative with respect to the argument and all functions are evaluated at $\eta(0) = (\omega_p/\alpha)^{2/3}$.

In the asymptotic limit $\alpha t \gg 1$ Eq (20) implies that the particle position is given by

$$x \approx (E_0/\alpha R) F \cos[(2\omega_p/3\alpha)(1+\alpha t)^{3/2} + \psi] / (1+\alpha t)^{1/4} \quad (22)$$

In Eq (22) ψ is a phase angle determined by the ratio of a to b, and F is the corresponding amplitude, which is strictly a function of $(\omega_p/\alpha)^{2/3}$.

It is seen from Eq (22) that the trapped particles execute rapid oscillations whose amplitude is proportional to the displacement of the bottom of the well produced by E_0 (i.e., Eq (3)). These oscillations decrease in time due to the compression produced by the ever increasing potential well. It is this compression which is responsible for the formation of the singular charge clumps associated with the dynamic BGK equilibrium described in Sec V. It should be noted that although Eq (22) applies exactly to a linearly increasing wave amplitude, similar results are obtained for other time dependences, and can be calculated asymptotically by means of the well known WKB analysis.

III. Weak Cold Beam Formalism

Consider a fast electron beam of initial speed v_0 whose density n_b and thermal spread are sufficiently small to meet the weak cold beam criteria.¹⁶ The beam is assumed to propagate through a medium (a cold plasma of density n_0 or an equivalent slow wave structure) whose behavior remains strictly linear, so that this contribution to the problem can be described analytically by means of a slowly varying dielectric $\epsilon[k, \omega(t)]$. Since in the present study one is interested in the role played by the dynamics of the trapped particles, the beam is discretized into N charge sheets whose individual orbits $x_j(t)$ are followed in a digital computer self-consistently with the evolution of the waves. This procedure is to be contrasted with the analytic description of the beam behavior used in the spatially averaged formalism.

Defining the scaled position of particle j in a frame moving with the initial velocity of the beam by $\xi_j(t) = k_0[x_j(t) - v_0 t]$, where k_0 is the wavenumber of the fastest growing linearly unstable wave, yields the equation of motion

$$\frac{d^2}{d\tau^2} \xi_j = \epsilon - \left\{ \sum_k A_k(\tau) \exp[i(\lambda_k \xi_j - \delta_k \tau)] + \text{c.c.} \right\} \quad (23)$$

where the scaled quantities are

$$\Omega = \left[\omega_p^2 (n_b/n_0) / (\partial \epsilon_r / \partial \omega)_0 \right]^{1/2}, \quad \tau = \Omega t$$

$$\lambda_k = k/k_0, \quad \delta_k = (\omega_k^0 - \omega_0 k/k_0) / \Omega$$

$$A_k = (ek_0/m\Omega^2) E_k, \quad \epsilon = (ek_0/m\Omega^2) E_0 \quad (24)$$

The physical meaning of the quantities in Eq (24) is the following. E_k is the complex amplitude of a wave having wavenumber k , which in the absence of the beam has a laboratory frequency $\omega_k^0 = \omega_p$, where ω_p is the electron plasma frequency of the background medium. A_k is the wave amplitude scaled to the saturation level $E_T = m\Omega^2 / ek_0$ due to beam trapping by the fastest growing wave k_0 , when $E_0 = 0$. Ω is essentially the growth rate of the linear beam-plasma instability, and τ is the appropriately normalized time variable. δ_k is the Doppler shifted frequency of mode k_0 in the frame moving with speed v_0 . ω_0^0 refers to the frequency of mode k_0 in the absence of the beam. Finally, ϵ_r is the real part of the dielectric, i.e., $\epsilon = \epsilon_r + i\epsilon_i$, and $(\partial\epsilon_r/\partial\omega)_0$ is the derivative evaluated at $k=k_0, \omega=\omega_0^0$. By analogy, $(\partial\epsilon_r/\partial\omega)_k$ refers to the same quantity evaluated at k and ω_k^0 .

The self-consistent time evolution of A_k is determined from Poisson's equation, which in the slow time scale approximation ($\Omega \ll \omega_p$) takes the form

$$\frac{d}{d\tau} A_k + \Gamma_k A_k = (D_k / N\lambda_k) \sum_{j=1}^N \exp \left\{ -i(\lambda_k \xi_j - \delta_k \tau) \right\} \quad (25)$$

in which

$$\begin{aligned} \Gamma_k &= (\epsilon_i / \Omega) / (\partial\epsilon_r / \partial\omega)_k \\ D_k &= (\partial\epsilon_r / \partial\omega)_0 / (\partial\epsilon_r / \partial\omega)_k \end{aligned} \quad (26)$$

Physically, Γ_k represents the weak dissipation acting on mode k . Its origin is left unspecified in the present work, but can be conceptually associated with background plasma heating, wall heating, radiation leakage, etc.

The principal dynamical effects associated with the presence of the external DC electric field can be understood from the exact conservation relations derivable from Eqs (23) and (25), namely

$$\frac{d}{dt} \left[\sum_j \frac{\dot{x}_j}{N} + \sum_k (\lambda_k / D_k) |A_k|^2 \right] = E - 2 \sum_k (\lambda_k / D_k) \Gamma_k |A_k|^2 \quad (27)$$

and

$$\begin{aligned} \frac{d}{dt} \left\{ \sum_j \frac{\dot{x}_j^2}{2N} + \sum_k D_k^{-1} [\delta_k + 2 \operatorname{Re}(s\omega_k)] |A_k|^2 \right\} \\ = E \left(\sum_j \frac{\dot{x}_j}{N} \right) - 2 \sum_k (\Gamma_k / D_k) [\delta_k + \operatorname{Re}(s\omega_k)] |A_k|^2 \end{aligned} \quad (28)$$

where, $\operatorname{Re}(\delta\omega_k)$ refers to the real part of the complex frequency shift defined by

$$A_k(\tau) = A_k(0) \exp \left[-i \int_0^\tau d\tau' s\omega_k(\tau') \right] \quad (29)$$

Equation (27) is the conservation law for the total momentum of the system, which is composed of the beam momentum

$$P_b = \sum_j \frac{\dot{x}_j}{N} \quad (30)$$

and the wave momentum

$$P_w = \sum_k (\lambda_k / D_k) |A_k|^2 \quad (31)$$

The total momentum can be altered (increased or decreased) by a nonzero \mathcal{E} , and is destroyed whenever there exists a wave dissipation channel (i.e., $\Gamma_k \neq 0$).

Equation (28) represents the conservation of energy principle in the frame moving with speed v_0 relative to the lab. It states that the total energy, composed of the mechanical beam energy

$$u_b = \sum_j \frac{\dot{\xi}_j^2}{2N} \quad (32)$$

and the wave energy

$$u_w = \sum_k D_k^{-1} [\delta_k + 2 \operatorname{Re}(s w_k)] |A_k|^2 \quad (33)$$

is altered by the work done on the beam particles by \mathcal{E} , and is dissipated when $\Gamma_k \neq 0$.

For $\Gamma_k = 0$, the conservation laws take the simple form

$$\frac{d}{d\tau} (P_b + P_w) = \mathcal{E} \quad (34)$$

$$\frac{d}{d\tau} (u_b + u_w) = \mathcal{E} P_b \quad (35)$$

When $\mathcal{E} = 0$, Eq (34) is satisfied by balancing the growth of the nearly monochromatic wave with a corresponding decrease in the beam momentum, i.e., the beam recoils. As the beam recoils, its kinetic energy increases in the frame moving with speed v_0 relative to the lab, thus Eq (35) is satisfied by the appear-

ance of a self-consistent real frequency shift of the single mode. The simultaneous constraints imposed by Eqs (34) and (35) result in the trapping of the beam particles and the corresponding saturation in the growth of the single mode.

For $E_0 \neq 0$, it is evident from Eqs (34) and (35) that a steady state does not exist. Both, the total momentum and the total energy of the system must increase secularly in time due to the external push. There are two conceptually different states capable of satisfying Eqs (34) and (35). One of them is the pure runaway regime, in which the external push provided by the DC field gives rise to an unbounded growth in beam momentum, i.e., $dp_b/dt \sim E_0$. The other state is the more subtle beam clamping regime, in which the beam momentum remains essentially constant while the wave amplitude increases secularly in time, i.e., $dp_w/dt \sim E_0$. Of course, one also encounters an intermediate state in which only a small fraction of the beam remains clamped, thus resulting in a simultaneous increase in mechanical and wave momentum.

The attainment of a given state, beam or wave runaway, is determined by the strength of the DC electric field. If $E_0 \gg E_T$, then the force produced by the wave can not cancel the external push, consequently the beam runaway regime is triggered. However, if $E_0 < E_T$, then the push of the external field can be reduced by the wave electric field. As is discussed in Sec II, the DC field shifts the position of the trapped particles relative to the bottom of the well, hence the particles continue to drive the wave unstable. Another way of visualizing this effect is to say that the DC field offsets the beam recoil associated with the saturation process for $E_0 = 0$. For $E_0 \sim E_T$ it is expected that the intermediate regime should set in.

IV. Clamping Behavior

To investigate the dynamics of beam clamping, Eqs (23) and (25) are solved numerically for a collection of discretized beam particles, typically in the range $N=300-500$. At first we consider the undamped ($\Gamma_k=0$) single mode problem in which the linearly fastest growing mode becomes dominant and traps the beam electrons.

In Fig. 2, the smaller curve, labelled $E_0=0$, exhibits the time evolution of the amplitude of the single mode when there is no DC electric field present. The characteristic long-lived amplitude oscillations due to the bouncing motion of the trapped particles are evident. The secularly growing solid curve in Fig. 2 is the result obtained by turning on a DC field of strength $E_0=0.5E_T$ at the time the wave reaches the first peak, i.e., at the saturation time. As predicted by the spatially averaged formalism and required by the conservation laws, the wave exhibits unbounded growth (wave runaway) while the momentum of the beam particles remains clamped (i.e., it does not increase). The dashed curve in Fig. 2 represents an approximate prediction that would be made by the spatially averaged formalism, i.e.,

$$A(\tau) \approx [A^2(\tau_0) + \epsilon(\tau - \tau_0)]^{1/2} \quad (36)$$

where, τ_0 refers to the turn-on time. Of course, the more sophisticated prediction of the spatially averaged theory would require the simultaneous solution of 3 algebraic equations, as is done in Ref. 10. Nevertheless, the simple prediction of Eq (36) gives a good account of the average secular growth induced by the DC field. However, Eq (36) can not reproduce the oscillations that accompany the secular growth. These oscillations are associated with the bouncing motion of the trapped particles in a potential well which grows in time, as described by

the analytic solution [Eqs (20) and (22)] of the model discussed in Sec II. As expected, Fig. 2 shows that the frequency of the amplitude oscillations increases, and their depth disappears.

Figure 3 displays the phase-space patterns at $\tau=35.0$ for the two cases shown in Fig. 2. Note that the velocity scales are different for the two cases, while the spatial scales are the same. In Fig. 3 the solid curve superimposed on the phase-space pattern is the instantaneous spatial dependence of the force produced by the wave. The major difference between the two cases is that for $E_0=0$, the trapped particles are smeared out over a full wavelength, whereas for $E_0 = 0.5E_T$ the particles are focused and exhibit a spiraling motion of ever decreasing spatial extent. It should be stressed that the average momentum of these particles does not increase even though the DC field is acting on them. In addition, the phase-space for $E_0 = 0.5E_T$ shows the existence of a secondary population of run-aways which consists of less than 10% of the original beam particles.

An element of potential weakness in the spatially averaged theory of clamping is the need to specify the spatially averaged distribution function $\langle f \rangle$ of the beam, as it interacts with the growing waves. The simplest mathematical choice is used in that formalism. It consists simply of a Lorentzian whose parameters change self-consistently with the conservation laws. The reason why the spatially averaged formalism is so successful in predicting the clamping behavior in spite of this difficulty is that the actual $\langle f \rangle$ obtained by following the exact particle orbits has the essential qualitative features of the Lorentzian beam, as can be seen in Fig. 4. It is observed in this figure that the majority of the particles form a clamped beam that has a finite thermal spread which increases slowly in time. Figure 4 also shows a feature which is completely missed by the spatially averaged theory, namely, a small secondary runaway beam which can not be stopped by the main wave. The secondary beam can interact with other modes having faster

phase velocities and may divide itself into a clamped component and yet another secondary beam. Therefore, a percolation process can be established in phase-space that produces a multiple beam distribution function of the type observed in a toroidal strong turbulence experiment.²²

The enhanced damping effect produced by reversing the direction of the DC field is shown in Fig 5a). In here, $E_0 = -0.5E_T$, hence the beam is decelerated out of resonance with the wave, i.e., the wave switches from the unstable slow beam root to the damped fast component, as is described by the spatially averaged theory. The originally trapped particles evolve into a decelerating beam whose phase-space structure is displayed in Fig 5b) for $\tau = 35.0$.

The time development of the pure beam runaway regime is exhibited in Fig. 6a) for $E_0 = 4.0E_T$; the $E_0 = 0$ is included for comparison. It is seen that the DC field initially enhances the wave amplitude above the normal saturation level due to the favorable relative displacement of the bottom of the potential well described previously. However, in this case the push given by the DC field is too strong and cannot be compensated by the enhancement in the wave amplitude. Accordingly, the trapped particles are pushed out of the wave troughs and become runaway electrons whose phase-space structure is shown in Fig 6b). The transition from trapped particles to runaways encountered in this problem is a classical analog of the process of ionizing an atom.

The clamping behavior exhibited in Fig. 2 has been obtained by turning on the DC field at the time of saturation for the single mode. Therefore, it is of interest to investigate if the attainment of this state depends crucially on this particular choice of timing. The result of such an investigation is shown in Fig. 7, where it is seen that the clamping state characterized by the secular increase in wave amplitude is attained over a wide choice of initial timing. The timing window sampled in Fig. 7 ranges from the pre-trapping stage (1) through

the damping (2-4) and regrowth (4-6) cycles of the dynamics. The principal effect associated with the choice of timing is the natural delay of the onset of the secular growth stage, which is manifested in Fig. 7 as the relative slippage of the wave amplitudes for the different cases (1-6).

The sensitivity of the clamping state to the amplitude of the applied DC electric field can be quantified by means of the ratio of the number of runaway electrons created N_R to the total number of initial beam particles N . The dependence of this ratio on E_0/E_T is displayed in Fig. 8. It is seen that for $E_0/E_T < 1.25$ the runaways constitute less than 10% of the total population and their number is not sensitive to the exact value of E_0 . The reason for this behavior is that in this regime a significant fraction of the runaways are created by the natural spillage of the trapped particles out of the time dependent potential wells; a process which occurs even when $E_0 = 0$. For $E_0 > 1.25E_T$, one observes a dramatic increase in the number of runaways, eventually attaining the 100% level at $E_0 = 4.0E_T$. This absolute upper limit on the destruction of trapping by a DC field is roughly a factor of 2 larger than expected for a wave of fixed amplitude. The reason for this higher threshold is that the wave amplitude grows due to the application of the DC field, hence the threshold discussed in Sec II (i.e., $E_0 = 2E_T$) varies as a function of time during the interaction. The net integrated result is essentially the curve shown in Fig 7.

Since the clamped state is insensitive to the timing of the DC field and it exists over a broad range of values $E_0 < 4.0E_T$, it is then possible to modulate the amplitude of the wave by applying DC pulses which are consistent with these limits. An example of such amplitude control is demonstrated in Fig 11, where one applies two square pulses of magnitude $|E_0| = 0.5E_T$, but having opposite polarity. It is seen that the amplitude can be increased, held constant, and decreased. An important point about such a control, which may have some practical application, is

that the response of the wave amplitude is essentially linear even though the dynamics of the underlying system is strongly nonlinear.

In the clamping behavior previously discussed, it is explicitly assumed that a single mode dominates the wave spectrum. In practice this situation can be realized if the system evolves from an extremely low noise level, or if the spectrum is initially enhanced by modulating the beam or launching a test wave of substantial amplitude and with a wavenumber corresponding to the fastest growing linearly unstable mode. The presence of many modes in the beam instability produces a natural smearing of the phase-space granulation associated with particle trapping. This effect can be viewed dynamically in terms of a non-stationary potential well (due to the sum over all modes) which gives rise to the stochastic trapping and detrapping of the resonant particles, or alternatively as arising due to global phase mixing because particles trapped in different troughs bounce with different phases and bounce frequencies. In either interpretation the net result is that the cold beam develops a thermal spread rather rapidly. Therefore, it is of interest to check if the secular wave growth triggered by the application of the DC electric field occurs in the more complicated multi-wave environment.

The role played by modes having wavelengths longer than that of the fastest growing mode (i.e., $k < k_0$) is shown in Fig 10. This figure exhibits the time evolution of the wave amplitudes of a system containing 7 modes. The spectrum consists of the fastest growing mode k_0 , and 6 lower modes having a mode spacing $\Delta k/k_0 = 0.07$, and with a beam density corresponding to $\Omega/\omega_p = 0.1$. In Fig 10a) the behavior for $E_0 = 0$ is shown. It is observed that the main mode is still dominant throughout the entire time evolution. However, the trapped particle amplitude oscillations are not well defined. The reason for this behavior is seen in the phase-space shown in Fig. 10 b), where a high degree of phase mixing is observed.

The effect produced by the application of a DC electric field ($E_0=0.5E_T$) to this system is shown in Fig. 11a). It is found that the characteristic secular growth in wave amplitude indeed occurs, and that clear trapping oscillations now become evident. Note the difference in amplitude scales between Figs. 10a) and 11a). As expected from Fig. 11a), the phase-space associated with the secular growth, Fig. 11b), shows heavily populated clumps and a negligible number of secondary runaways, quite similar to the behavior obtained for the pure single mode case.

The effect produced by the inclusion of waves having wavelengths shorter than that of the main mode (i.e., $k > k_0$) is shown in Fig 12a). The spectrum in this system contains the fastest growing mode k_0 , and two upper and two lower sidebands with mode spacing $\Delta k/k_0=0.08$, and $\Omega/\omega_p=0.1$. The principal feature in this system is that the main mode decays right after reaching saturation and triggers the growth of an upper sideband which eventually dominates the spectrum. In this case the characteristic trapping oscillations are absent, as is expected from the corresponding phase-space shown in Fig 12b). The application of a DC electric field ($E_0=0.7E_T$) to this system also produces a secular growth in the wave amplitude, as shown in Figure 13a). Again, note the change in scales between Figs 12a) and 13a). The degree of clump formation in this case is much less than in the pure single mode problem and the number of secondary runaways is significantly increased as seen in the phase-space of Fig 13b). The reason for this behavior is that in the zero order system ($E_0=0$), particle trapping is destroyed by the sideband growth.

V. Dynamic BGK Equilibrium

It has been shown in the previous section that in the absence of dissipation the wave amplitude exhibits unbounded growth for DC fields such that $E_0 < 4.0E_T$. Within the restrictions of the model a steady state cannot be attained. Therefore, the clamped beam particles are compressed into singular charge clumps. However, when a finite amount of wave dissipation is present, an interesting nonlinear steady state can be found analytically. It consists of a trapped particle equilibrium of the type associated with a BGK mode, but in which there is energy and momentum being continuously circulated through the system.

The steady state flow of energy and momentum can be deduced from Eqs (27) and (28) for the single mode problem, i.e.,

$$\frac{d}{dt} [P_b + P_w] = E - 2\Gamma |A|^2 \quad (37)$$

$$\frac{d}{dt} [u_b + u_w] = E P_b - 2\Gamma W |A|^2 \quad (38)$$

where Γ is the damping rate, W the real frequency shift and A the wave amplitude. The steady state is obtained by balancing the dissipation of energy and momentum due to the wave damping against the source of momentum and energy provided by the DC field. The requirements are

$$A = (E/2\Gamma)^{1/2}, \quad W = P_b \quad (39)$$

These conditions arise from global properties of the wave-particle system and must be consistent with the motion of the individual particles in order for the steady

state to be realizable. To check this consistency requirement, write the equation of motion for particle j in real form

$$\frac{d^2}{d\tau^2} \xi_j = E - 2A(\tau) \cos \left[\xi_j(\tau) - \int_0^\tau d\tau' W(\tau') \right] \quad (40)$$

from which it is seen that $dp_b/d\tau=0$ if the particle position is given by $\xi_j(t) = \theta + p_b \tau$. In here θ is a constant phase factor independent of the particle label j (i.e., a singular charge clump is formed), and must satisfy the force equilibrium condition

$$\frac{E}{2A} = \cos \theta \quad (41)$$

which has a physical solution provided $E/2A < 1$. This consistency requirement, together with Eq (39), implies that $(E \Gamma/2)^{1/2} < 1$ for the dynamic BGK equilibrium to exist.

It must then be verified that the choice of a singular clump indeed gives rise to a constant wave amplitude and a constant frequency shift. This check can be obtained by analyzing the real version of Eq (25), namely

$$\frac{d}{d\tau} A + \Gamma A = \frac{1}{N} \sum_j \cos \left[\xi_j - \int_0^\tau d\tau' W(\tau') \right] \quad (42)$$

$$AW = \frac{1}{N} \sum_j \sin \left[\xi_j - \int_0^\tau d\tau' W(\tau') \right] \quad (43)$$

The choice of a singular clump population transforms Eq (42) into

$$\frac{d}{d\tau} A + \Gamma A = \cos \theta \quad (44)$$

which using the dynamical equilibrium condition of Eq (41), together with the conservation constraints of Eq (39), results in

$$\frac{d}{d\tau} A + \Gamma A = (2\Gamma A^2)/2A \quad (45)$$

thus showing that $dA/d\tau=0$, as required.

Similarly, Eq (43) is transformed into

$$W = \sin \theta / A \quad (46)$$

which is explicitly time independent in view of Eq (45), and from which one obtains the self-consistent frequency shift associated with the dynamic BGK equilibrium

$$W = - (2\Gamma/\epsilon)^{1/2} [1 - (\epsilon\Gamma/2)]^{1/2} \quad (47)$$

The choice of the negative sign in the square root of Eq (47) is determined by the physical need to locate the clump within the confining trough of the wave potential. The disregarded positive root corresponds to a potential hill instead of a valley.

The nonlinear steady state analyzed in this section consists of a singular charge clump which is located inside the potential trough of a constant amplitude wave and propagates at constant speed even though an external DC electric field

acts on it. This is an example of a nonlinear dynamical equilibrium in which the trapped beam particles play the role of an intermediate agent which transfers the external momentum push of the DC electric field to those physical mechanisms responsible for the wave damping. The physics behind the continuous excitation of the wave is that the constant position of the charge clump is displaced relative to the bottom of the wave trough in the positive energy transfer phase of the usual trapped particle energy transfer cycle, as is evident from Eq (44).

The singular charge clump associated with the dynamic BGK equilibrium can be attained only in the limit $\Gamma \rightarrow 0$, $\tau \rightarrow \infty$ (neglecting space charge limits, which eventually become important). For finite values of Γ and τ , the actual clump has a finite spatial extent. The consequence of not having a perfect charge singularity on the parameters of the exact dynamic BGK equilibrium can be assessed by expressing the orbit of the j trapped particle as

$$\xi_j = \xi_0 + W\tau + \alpha_j \cos(\beta_j \tau + \phi_j) \quad (48)$$

where ξ_0 is the force free equilibrium position defined by $\cos \xi = E/2A$, and α_j is the finite excursion having frequency β_j and random phase ϕ_j .

Considering that a fraction $\sigma < 1$ of the original beam particles remain clamped and a corresponding amount $(1 - \sigma)$ runs away, as is always the case, implies that the self-consistent frequency and amplitude are determined essentially by

$$\Gamma A = \frac{\sigma}{N} \sum_j \cos[\xi_0 + \alpha_j \cos(\beta_j \tau + \phi_j)] \quad (49)$$

$$W A = \frac{\sigma}{N} \sum_j \sin[\xi_0 + \alpha_j \cos(\beta_j \tau + \phi_j)] \quad (50)$$

in which the small (high frequency) modulation due to the oscillatory orbits of the runaways, given in Eq (13), is neglected.

Using the finite series expansion in terms of Bessel functions for the expressions in Eqs (49) and (50), and realizing that summing over j is equivalent to averaging over the random phases ϕ_j leads to

$$\Gamma A = f \cos \xi_0 \quad (51)$$

$$W A = f \sin \xi_0 \quad (52)$$

$$f = \frac{\sigma}{N} \sum_j J_0(\alpha_j) \quad (53)$$

where J_0 is the Bessel function of order 0 and the quantity f measures the degree of focusing of the clump, e.g., as $\alpha_j \rightarrow 0$, $f \rightarrow \sigma$.

Solving Eqs (51) and (52) leads to the modified parameters for the approximate BGK equilibrium due to a finite size clump

$$A = (f \epsilon / 2 \pi)^{1/2} \quad (54)$$

$$W = - (2 \pi f / \epsilon)^{1/2} [1 - (\pi \epsilon / 2 f)]^{1/2} \quad (55)$$

which reduce to Eqs (39) and (47) in the limit $f=1$. From Eq (55) one finds the more restrictive condition for the existence of the finite size BGK equilibrium to be $(\pi \epsilon / 2) \leq f$. This condition should be used in conjunction with Fig 8 to delineate the parameter space amenable to the formation of a dynamic BGK equilibrium.

To check on the existence of the dynamic BGK equilibrium, we solve Eqs (23) and (25) as in Sec IV, but now proceed to include the effect of damping, i.e., $\Gamma \neq 0$. Figure 14a) shows the time evolution of the wave amplitude for the case $\Gamma = 0.02$, $E_0 = 1.0 E_T$. It is found now that the secular behavior, exemplified by Fig. 2, is stopped. The system approaches asymptotically a steady state whose amplitude is slightly smaller than the prediction of Eq (39), i.e., $(\epsilon/2\Gamma)^{1/2} = 4.2$. Simultaneously with the approach to this steady state, one observes the formation of a high density cluster of beam particles, a clump, whose velocity remains essentially constant, as is characteristic of the dynamic BGK equilibrium, and is exhibited in the phase-space plot of Fig 14b).

The formation of a highly coherent trapped particle state in the presence of finite damping, as demonstrated in Fig. 14, may on first thought appear to contradict the well documented fact that trapping can be destroyed due to the effect of finite damping, as studied by Dimonte and Malmberg.⁸ As shown by these authors, the destruction of trapping is not due to the obvious dissipative decrease in wave amplitude, but rather it is caused by a sudden nonlinear phase shift which pulls the particles out of the wave troughs, thus causing a dramatic damping in the wave amplitude. Figure 15 shows the existence of this sudden damping, for $\Gamma = 0.075$, occurring just after the second trapped particle oscillation, $\tau < 20.0$. The phase-space structure corresponding to this damping is shown in Fig. 16a), where it is evident that strong phase mixing has occurred. The effect produced by the application of a DC electric field to the phase-space structure of Fig 16a) is exhibited in the late time ($\tau > 30$) portion of Fig 15. The DC field causes the regrowth of the wave and asymptotically it approaches a dynamic BGK equilibrium. The regrowth of the wave is accomplished by the reorganization of the phase-space structure due to the push provided by the DC field. The DC push positions the majority of the

trapped particles in the correct phase for transferring energy to the wave, as seen in the phase-space of Fig 16b). In the process of moving the trapped particles to the favorable position for wave growth a secondary runaway population is created.

The attainment of a steady state due to finite wave dissipation in the presence of many modes is also possible, as shown in Fig. 17a) for the parameters $E_0 = 0.7E_T$, $\Gamma = 0.02$. The system contains 6 lower modes ($k < k_0$) in addition to the main mode, and has a mode spacing $\Delta k/k_0 \approx 0.07$ with $\Omega/\omega_p = 0.1$, as in the case considered earlier in Fig. 12. Together with the approach to an asymptotic constant wave amplitude, one observes in the corresponding phase-space picture of Fig. 17b) that spatially focused charge clumps appear, as expected from the dynamic BGK equilibrium analysis. However, due to the presence of several non-resonant modes, a significant fraction of secondary runaways is created. Since the runaways do not contribute to driving the wave amplitude, it is found that the asymptotic wave amplitude attains a level $A=3.0$ which is lower than the ideal pure single mode prediction of $A=4.2$. From this difference it can be estimated through Eq (54) that the focusing parameter has a value $f=0.56$. This value, although lower than that for a perfect dynamic BGK equilibrium ($f=1.0$), is found to satisfy the necessary existence criterion for the steady state, i.e., $\Gamma/2 < f$. A similar result is also obtained when upper sidebands as well as lower sidebands are present. However, due to the destruction of particle trapping produced by the upper sidebands, as seen in Fig. 12, the degree of clumping is significantly reduced, i.e., the focusing parameter attains a low value $f=0.2$.

VI. Stability of Clump Equilibrium

Several years ago considerable theoretical effort was devoted to the study of the sideband instability associated with trapped particle BGK equilibria. The motivating reason for the intensive theoretical activity was the experimental observation of Wharton, et al.²³ that sideband signals were spontaneously excited when a monochromatic large amplitude electron plasma wave was externally launched in a collisionless plasma. One of the more interesting models proposed to explain the experimental results was advanced by Kruer, et al.²⁴ It consisted of the ad-hoc assumption that the trapped particles were bunched into a singular clump located exactly at the bottom of the potential well of the wave. The earliest analysis of this model by Kruer, et al. showed that sideband waves were indeed unstable; the physics behind the instability being essentially associated with the linear dynamics of a spatially periodic cold beam. Although a computer particle simulation²⁵ of the problem by Kruer, et al. showed that instead of a singular clump, a large hole was formed at the bottom of the well, the clump model yielded predictions which were in rough agreement with the observed sideband growth. The analysis of Kruer, et al. was subsequently corrected by Goldman and Berk²⁶ to include the important effect produced by the requirement of self-consistency, i.e., a nonlinear frequency shift must always accompany the formation of the charge clumps. The nonlinear frequency used by Goldman and Berk was taken from an early calculation by Bohm and Gross²⁷, and although it provides a logical improvement upon the model of Kruer, et al., it is not the correct frequency shift^{5,6} associated with a large amplitude electron plasma wave. These difficulties simply stem from the fact that the clump model is not the correct dynamical description of the launched wave problem. Nevertheless, it is an interesting system to investigate.

The dynamic BGK equilibrium discussed in Sec V has the singular clump nature of the model postulated by Kruer, et al., but does not suffer from the lack of self-consistency and dynamical origin. The wave amplitude, clump position, and nonlinear frequency shift are all analytically known. In addition, the formation of the clump is dynamically possible due to the spatial compression provided by the secular growth of the wave potential. Accordingly, the dynamic BGK equilibrium is the natural system for calculating the stability of clump equilibria.

The stability analysis that determines the growth of small waves of amplitude \tilde{E} , wavenumber k , and frequency ω , can be performed in a manner analogous to the calculation of Kruer, et al. The result is

$$\epsilon(k, \omega) \tilde{E}(k, \omega) = \frac{\sigma \omega_p^2 (n_b/n_0)}{(\omega - k \bar{v}_0)^2 - \bar{\omega}_b^2} \sum_{l=-\infty}^{\infty} \tilde{E}(k + l k_0, \omega + l k_0 \bar{v}_0) \exp(i l \xi_0) \quad (56)$$

in which \bar{v}_0 refers to the time asymptotic velocity of the wave (different from v_0), and $\bar{\omega}_b$ is the bounce frequency in the presence of the DC electric field given by Eq (10).

In general, the stability problem involves the solution of an infinite determinant which represents the coupling of all the Floquet (Bloch) states $k + l k_0$, as indicated in Eq (56). However, in the limit of small n_b/n_0 the lowest order nontrivial coupling which is often investigated consists of retaining only the $l=0,2$ terms. The simplified system consists of

$$\begin{vmatrix} \epsilon(1) + I_T & , & I_T \exp(-i \xi_0) \\ I_T \exp(i \xi_0) & , & \epsilon(2) + I_T \end{vmatrix} = 0 \quad (57)$$

where $\epsilon(1)=\epsilon(k,\omega)$, $\epsilon(2)=\epsilon(k-2k_0,\omega-2k_0\bar{y}_0)$, and

$$\chi_T = -\frac{\sigma\omega_p^2(n_b/n_0)}{(\omega - k\bar{v}_0)^2 - \bar{\omega}_b^2} \quad (58)$$

The expansion of Eq (57) leads to the dispersion relation

$$1 = -\chi_T \left[\frac{1}{\epsilon(1)} + \frac{1}{\epsilon(2)} \right] \quad (59)$$

which has the characteristic structure of a parametric instability problem.

Taking into consideration that $\omega=\omega_p+\delta\omega$, $|\delta\omega| \ll \omega_p$, and recalling the weak cold beam scaling given in Eqs (24) and (26) reduces Eq (59) to

$$(y - i\tau)(2W - y + i\tau) = \frac{\sigma W}{(y + \tau)^2 - \bar{\omega}_b^2} \quad (60)$$

in which the unknown complex frequency has been scaled to $y=\delta\omega/\Omega$, and the k dependence enters through

$$\tau = (1 - k/k_0)(\omega_p/\Omega) - (k/k_0)W \quad (61)$$

It should be mentioned that in arriving at Eq (60), the background plasma has been taken to be cold, hence the scaling factor $\Omega=\omega_p(n_b/2n_0)^{1/3}$.

The factor W appearing in Eq (61) is the self-consistent nonlinear frequency shift given by

$$W = - (2\tau\sigma/\epsilon)^{1/2} [1 - (\tau\epsilon/2\sigma)]^{1/2} \quad (62)$$

and the scaled bounce frequency is

$$\bar{W}_b = (2\sigma\epsilon/r)^{1/4} [1 - (r\epsilon/2\sigma)]^{1/4} [1 - (\epsilon r/32\sigma)] \quad (63)$$

The principal features of the dispersion relation, Eq (60), can be obtained by considering the limit $|W| \rightarrow 0$, $\bar{W}_b > 1$. Physically, this regime corresponds to weak damping and large potential wells, as is required for the formation of a dynamic BGK equilibrium. Neglecting the explicit dependence on r and W in the left side of Eq (60) yields

$$y^2 = \frac{\sigma |W|}{(y + r - \bar{W}_b)(y + r + \bar{W}_b)} \quad (64)$$

which shows that as $|W| \rightarrow 0$ the regions of instability are centered around $r = \pm \bar{W}_b$. Considering each of these regions to be well separated from each other results in

$$y^2(y + s_{\pm}) = \pm \sigma |W| \quad (65)$$

where $r = s_{\pm} \pm \bar{W}_b$. One can now define the useful scaled variable

$$z = (y + s_{\pm}) / (\sigma |W| / 2 \bar{W}_b)^{1/3} \quad (66)$$

to express Eq (65) in terms of a dispersion relation which is identical to that of the weak cold beam-plasma instability

$$z(z - \kappa_{\pm})^2 = \pm 1 \quad (67)$$

with $\kappa_{\pm} = s_{\pm} / (|W| \sigma / 2 \bar{W}_b)^{1/3}$. As is well known, the maximum growth rate in Eq (67) occurs for $\kappa_{\pm} = 0$, and has growing roots given by $z_{\pm} = \exp(i2\pi/3)$ for $r = +\bar{W}_b$, and $z_{\pm} = \exp(i\pi/3)$ for $r = -\bar{W}_b$. This implies that the maximum growth rate of the instability is

$$\max(\text{Im } \gamma) \approx (0.866) (\sigma |W| / 2 \bar{W}_b)^{1/3} \quad (68)$$

and corresponds to two growing sidebands

$$k_{\pm} = k_0 \left(\frac{1 \mp \bar{W}_b}{1 + \Omega W / \omega_p} \right) \quad (69)$$

centered around the main carrier mode k_0 , and each having a spectral width

$$\Delta k / k_0 \sim (\sigma |W| / 2 \bar{W}_b)^{1/3} \quad (70)$$

Using the self-consistent values for W and \bar{W}_b given in Eqs (62) and (63), yields the parametric dependence of the growth rate γ from Eq (68), namely

$$\gamma / \omega_p \approx (0.866) (\sigma \Gamma / \epsilon)^{1/4} (n_b / n_0)^{1/3} \quad (71)$$

This result shows that the sideband instability driven by the charge clumps associated with the dynamic BCK equilibrium disappears asymptotically as $\Gamma/\epsilon \rightarrow 0$. For finite values of $\Gamma/$, two growing sidebands appear at the bounce wavenumber $(k_b)_\pm = k_0 (2\epsilon/\Gamma)^{1/4}$.

The existence of these two unstable sidebands is illustrated in Fig 18, which is obtained by the exact numerical solution of the dispersion relation, Eq (60), for the parameters $\Gamma=0.02$, $\epsilon=1.0$, $\alpha=1$. The location of the sidebands coincides with the prediction $(k_b)_+ = (1.3)k_0$, $(k_b)_- = (0.7)k_0$. However, the maximum growth rate obtained (~ 0.25) is slightly smaller than that predicted by Eq (68) (i.e., ~ 0.31). The difference can be traced to the fact that the term $2|W| \approx 0.4$, hence it is not negligible in the left side of Eq (60), as is assumed in generating Eq (68), which is strictly correct in the limit $|W| \rightarrow 0$.

VII. Conclusions

This study has demonstrated that the phenomenon of beam clamping, predicted by the spatially averaged formalism, indeed occurs when the exact microscopic dynamics of the beam particles are calculated self-consistently. The clamping in beam energy produces an unbounded increase in wave amplitude. Therefore, the spatial structure associated with beam clamping (and averaged out in the previous formalism) corresponds to trapped particles which are strongly focused in space due to the large growing potential wells. This process can have practical applications in the areas of efficiency enhancement of travelling wave tube devices and future free electron lasers.

The limits on the amplitude of the DC fields which can be applied before runaway behavior sets in have been found. A useful insensitivity of the wave amplitude enhancement on the time of application of the DC field has been demonstrated.

In the presence of wave dissipation a new nonlinear state has been found analytically, and is observed to be approached in the time asymptotic limit by the numerical solutions of the problem. This state is a dynamic BGK equilibrium consisting of a singular charge clump which propagates through the medium at constant speed even though a DC electric field acts on it. The clump plays the role of an intermediate agent which transfers the external push to the sources responsible for the wave dissipation.

The dynamic BGK equilibrium found in this work provides the ideal analytical model to investigate the sideband instability triggered by trapped clumps, i.e., all its parameters are known analytically and it can be generated dynamically. The growth rate for this instability has been found.

In summary, a variety of interesting effects have been shown to arise when a DC electric field is applied to a system containing trapped particles. Many

of these effects appear to be readily amenable to experimental observation, and some may find a practical application.

ACKNOWLEDGMENTS

The author wishes to thank Dr. G. Dimonte for many useful discussions about this topic, and M. Thaker and I. Jechart for handling the computer programming tasks in a most professional manner.

This work has been supported by the Office of Naval Research.

Bibliography

1. R. K. Mazitov, Zh. Prikl. Mehkan. Tekh. Fiz. 1, 27(1965).
2. T. M. O'Neil, Phys. Fluids, 8, 2255(1965).
3. J. H. Malmberg and C. B. Wharton, Phys. Rev. Lett. 19, 775(1967).
4. N. Sato, H. Izeki, Y. Yamashita, and N. Takahashi, Phys. Rev. Lett. 20, 837(1968).
5. G. J. Morales and T. M. O'Neil, Phys. Rev. Lett. 28, 417(1972).
6. P. J. Vidmar, J. H. Malmberg, and T. P. Starke, Phys. Fluids 19, 32(1976).
7. I. B. Bernstein, J. Greene, and M. D. Kruskal, Phys. Rev. 108, 546 (1957).
8. G. Dimonte and J. H. Malmberg, Phys. Fluids 21, 1188 (1978).
9. R. N. Franklin, J. M. Hamberger, H. Izeki, G. Lampis, and G. J. Smith, Phys. Rev. Lett. 28, 1114(1972).
10. G. J. Morales, Phys. Fluids 22, 1359(1979).
11. C. Menyuk, D. Hammer, and G. J. Morales, Bull. Am. Phys. Soc. 22, 1200 (1977).
12. D. Hammer, N. C. Luhmann, and G. J. Morales, Bull Am. Phys. Soc. 22, 1201 (1977).
13. G. J. Morales, Phys. Rev. Lett. 41, 646(1978).
14. G. J. Morales, G. Dimonte, and M. T. Thaker, Bull. Am. Phys. Soc. 23, 817 (1978).
15. I. N. Onishchenko, A. R. Liveskii, M. C. Matsiborko, V. D. Shapiro, and V. I. Shevchenko, Pis'ma Zh. Eksp. Teor. 12, 407(1970) [JETP Lett. 12, 281(1970)]
16. T. M. O'Neil, J. H. Winfrey, and J. H. Malmberg, Phys. Fluids, 14, 1204 (1971).
17. K. W. Gentle and J. Lohr, Phys. Fluids 16, 1464(1973).

18. R. L. Hess, Ph.D dissertation, Electrical Engineering Department, University of California, Berkeley, May 1960 (unpublished).
19. A. T. Lin, and J. M. Dawson, Phys. Rev. Lett. 42, 1670 (1979).
20. N. Kryloff and N. Bogoliuboff, "Introduction to Nonlinear Mechanics," Princeton University Press, (1947).
21. "Handbook of Mathematical Functions," edited by M. Abramowitz and I. A. Stegun, Dover Publications, p.-227.
22. K. W. Gentle, G. Leifeste, and R. Richardson, Phys. Rev. Lett. 40, 317(1978).
23. C. B. Wharton, J. H. Malmberg, and T. M. O'Neil, Phys. Fluids 11, 1761 (1968).
24. W. L. Kruer, J. M. Dawson, and R. D. Sudan, Phys. Rev. Lett. 23, 838(1969).
25. W. L. Kruer, Ph.D dissertation, Department of Astrophysical Sciences, Princeton University, April 1969. (unpublished)
26. M. V. Goldman and H. L. Berk, Phys. Fluids 14, 801(1971).
27. D. Bohm and E. P. Gross, Phys. Rev. 75, 1851, 1864(1949).

Figure Captions

Fig. 1: Spatial Dependence of the effective trapping well in the presence of a DC field for the cases $E_0/A=0, 0.2, 0.5, 0.9$.

Fig. 2: Secular growth of wave amplitude produced by a DC field $E_0=0.5E_T$. The $E_0=0$ curve is the saturated beam instability in the absence of the DC field. The dashed curve is the approximate prediction based on conservation of momentum alone.

Fig. 3: Phase-space at $\tau=35.0$ for a) $E_0=0.5E_T$ and b) $E_0=0$. The solid curves represent the instantaneous spatial dependence of the wave force.

Fig. 4: Spatially averaged velocity distribution function in the clamped stage ($\tau=40.0$) for $E_0=0.5 E_T$. Note the appearance of a small secondary runaway component.

Fig. 5: Enhanced wave damping produced by a decelerating electric field. a) Time evolution of wave amplitude for $E_0=0$ and $E_0=-0.5E_T$. b) Phase-space at $\tau=35.0$ for $E_0=-0.5E_T$.

Fig. 6: Runaway beam regime. a) Time evolution of wave amplitude for $E_0=0$ and $E_0=4.0E_T$. b) Phase-space at $\tau=35.0$.

Fig. 7: Dependence of secular growth of wave amplitude on turn-on time of DC field. Inset shows turn-on time relative to $E_0=0$ evolution. Labels on secularly growing curves correspond to inset timing marks.

Fig. 8: Dependence of secondary runaway production on strength of DC field.

Fig. 9: External control of wave amplitude by two square-wave pulses of opposite polarity, $E_0=\pm 0.5E_T$.

Fig. 10: Effect of lower sidebands ($k < k_0$) for $E_0=0$. a) Time evolution of wave amplitude for 7 modes, $\Delta k/k_0=0.07$. b) Phase-space at $\tau=28.0$.

Fig. 11: Induced secular growth in the presence of lower sidebands ($k < k_0$) for $E_0=0.5E_T$. a) Time evolution of wave amplitude for 7 modes, $\Delta k/k_0=0.07$. b) Phase-space at $\tau=26.0$. To be compared with Fig. 10.

Fig. 12: Effect of lower ($k < k_0$) and upper ($k > k_0$) sidebands for $E_0=0$. a) Time evolution of wave amplitudes for 5 modes (two upper and two lower sidebands), $\Delta k/k_0=0.08$. b) Phase-space at $\tau=26.0$.

Fig. 13: Induced secular growth in the presence of lower ($k < k_0$) and upper ($k > k_0$) sidebands for $E_0=0.7E_T$. a) Time evolution of wave amplitudes for 5 modes (two upper and two lower sidebands), $\Delta k/k_0=0.08$. b) Phase-space at $\tau=0.02$. To be compared with Fig. 12.

Fig. 14: Time asymptotic approach to a dynamic BGK equilibrium in the presence of dissipation, $E_0 = 0.7E_T$, $\Gamma = 0.02$. a) Time evolution of wave amplitude. Theoretical prediction of steady state amplitude is $A = 4.2$. b) Phase-space at $\tau = 26.0$.

Fig. 15: DC field reversal of the destruction of trapping oscillations caused by finite dissipation. $\Gamma = 0.075$, $E_0 = 0.5E_T$. Sudden destruction occurs at $\tau = 18.0$, E_0 is applied at $\tau = 28.0$.

Fig. 16: Phase-space structures for a finite damping case $\Gamma = 0.075$ a) Subsequent to sudden damping, $\tau = 22.0$, $E_0 = 0$. b) After DC electric field is applied, $E_0 = 0.5E_T$, $\tau = 49.0$.

Fig. 17: Time asymptotic approach to dynamic BGK equilibrium in the presence of lower sidebands ($k < k_0$), $E_0 = 0.07E_T$, $\Gamma = 0.02$. a) Time evolution of wave amplitudes for 7 modes, $\Delta k/k_0 = 0.07$. b) Phase-space at $\tau = 36.0$.

Fig. 18: Scaled growth rate Y_I and frequency shift Y_R for unstable sidebands triggered by dynamic BGK equilibrium defined by $E_0 = 1.0E_T$, $\Gamma = 0.02$, $\sigma = 1.0$.

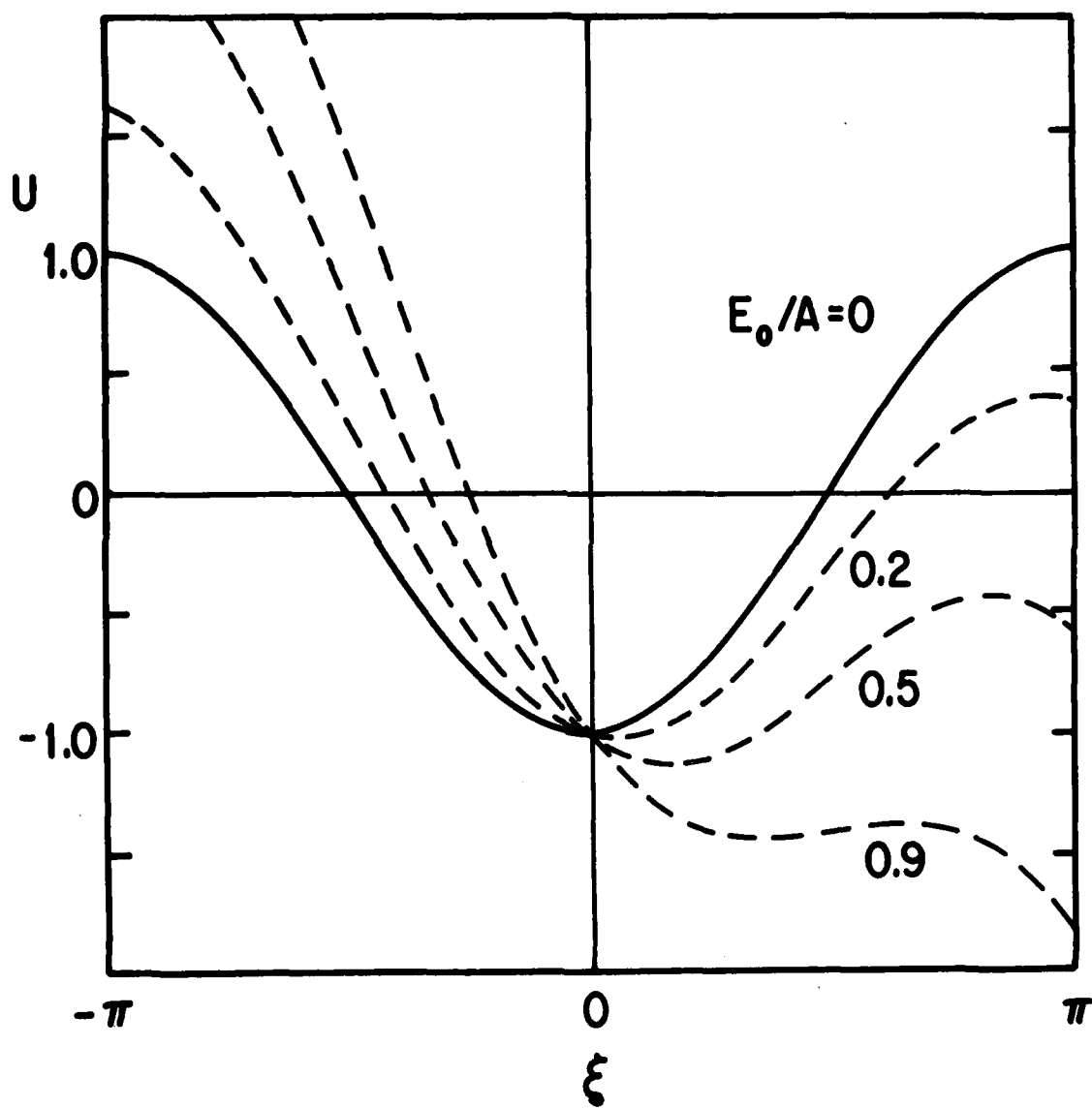


Fig. 1

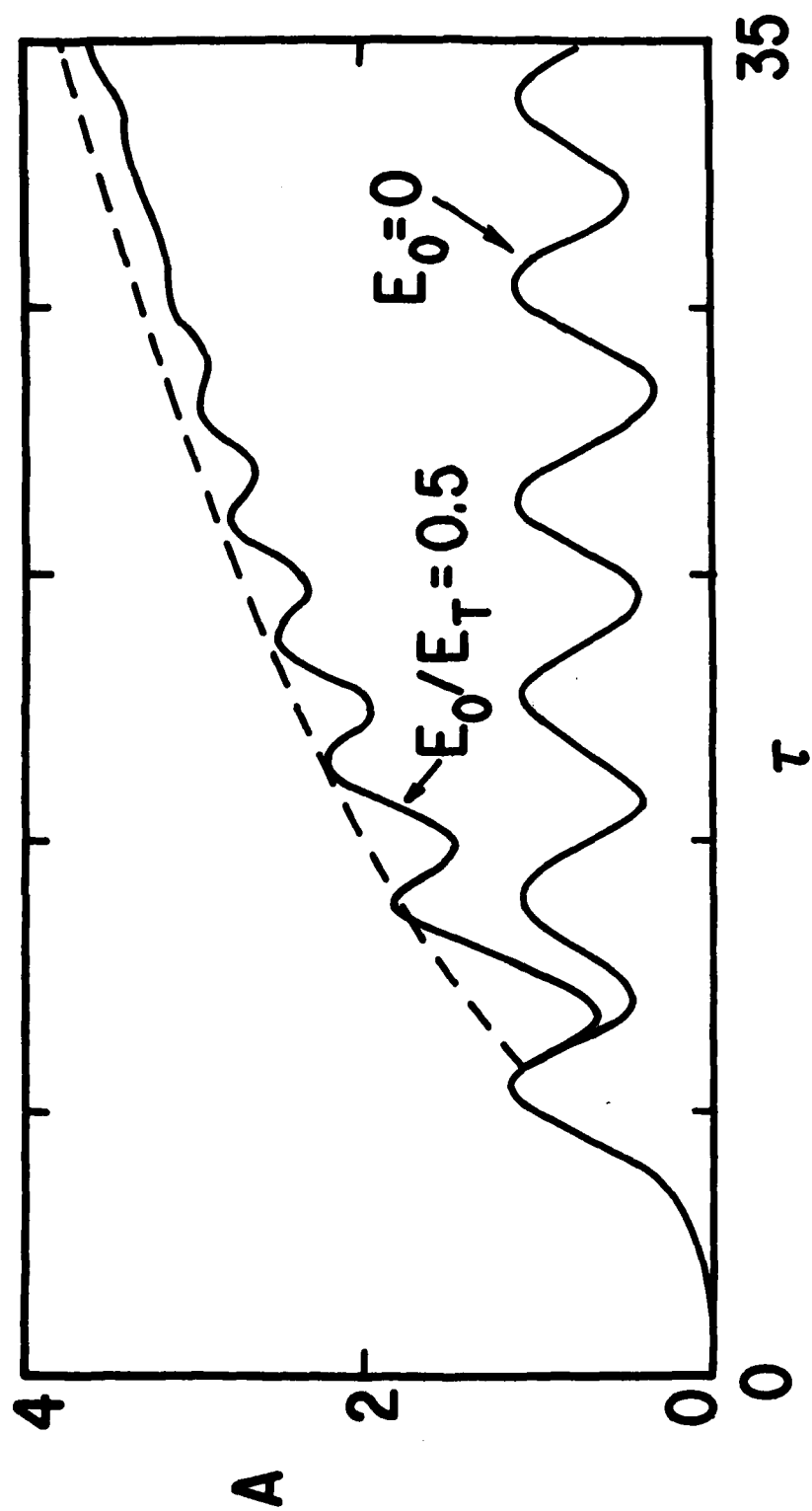


Fig. 2

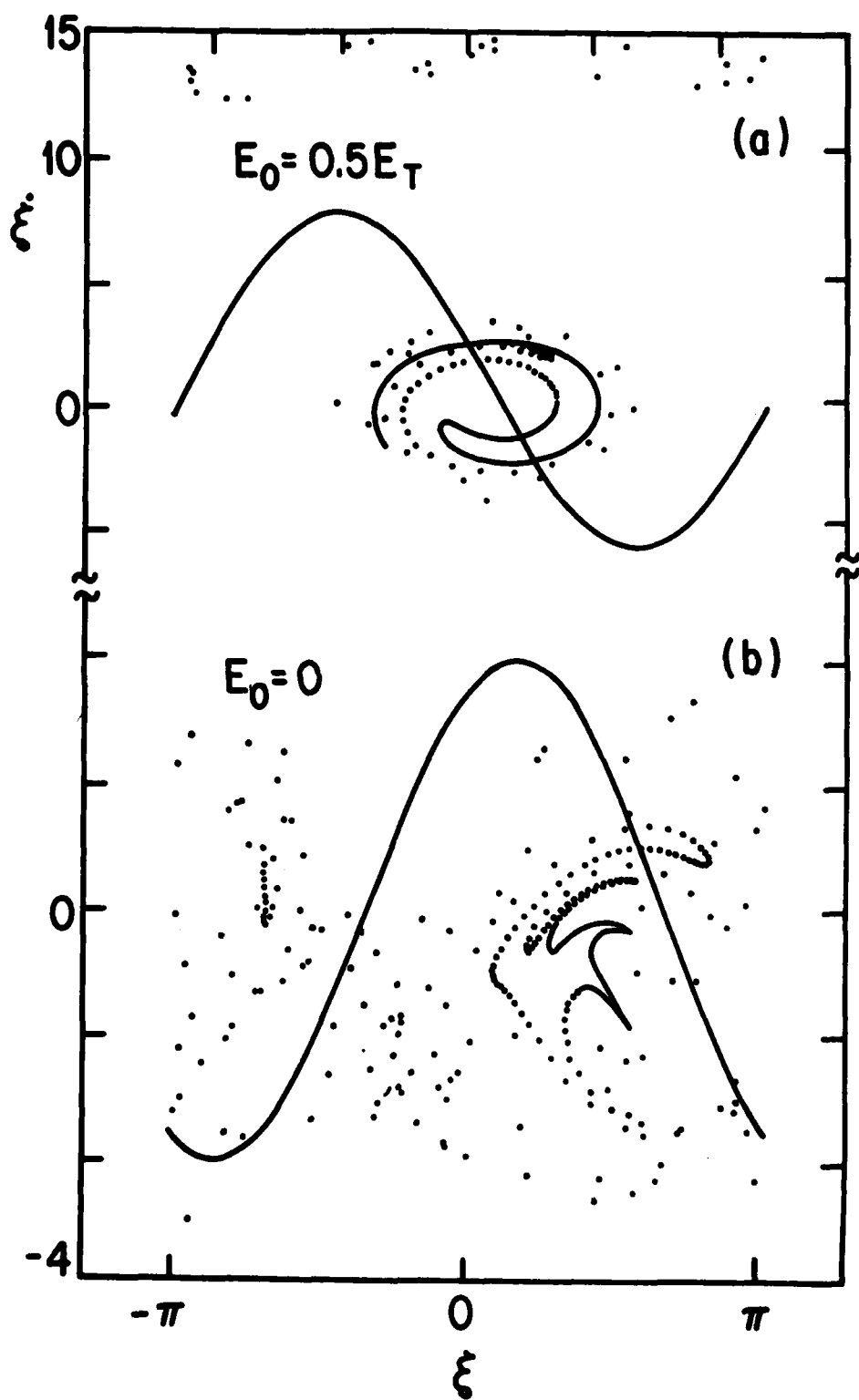


Fig. 3

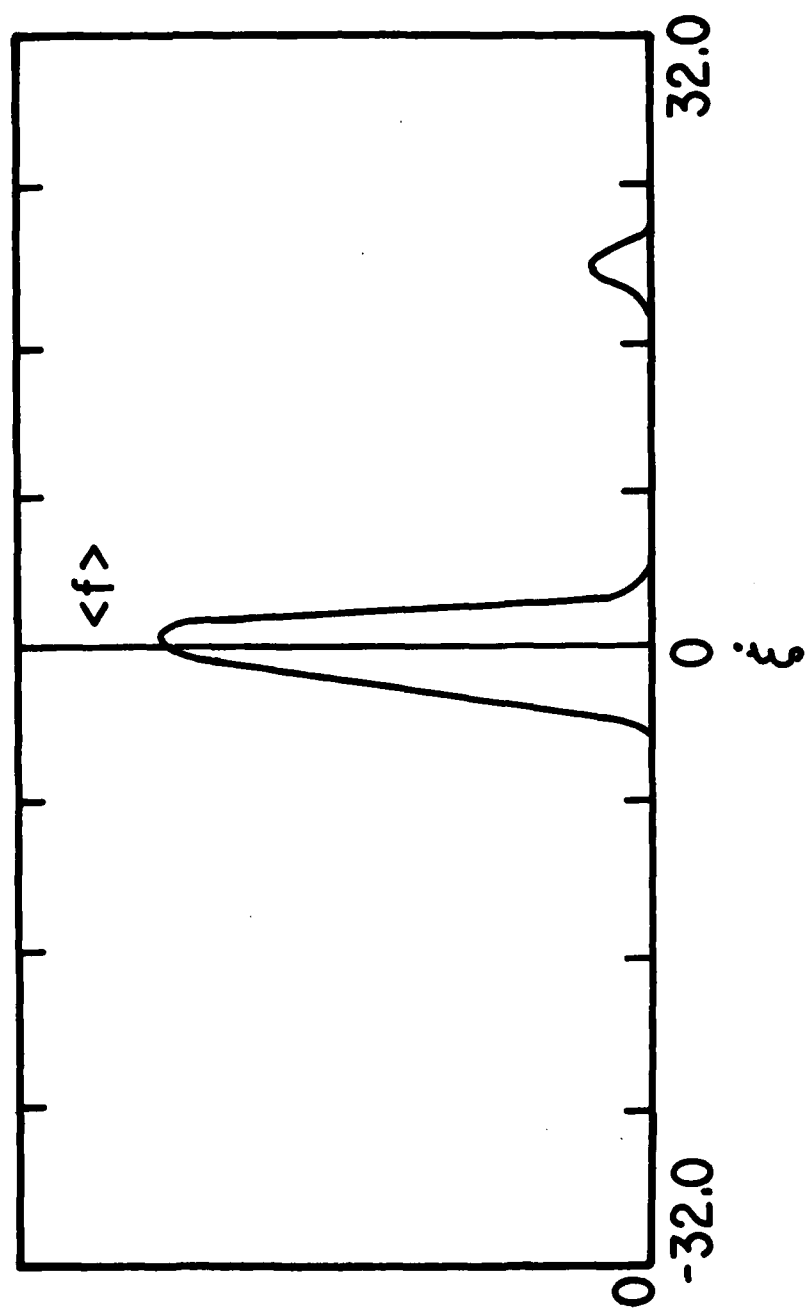


Fig. 4

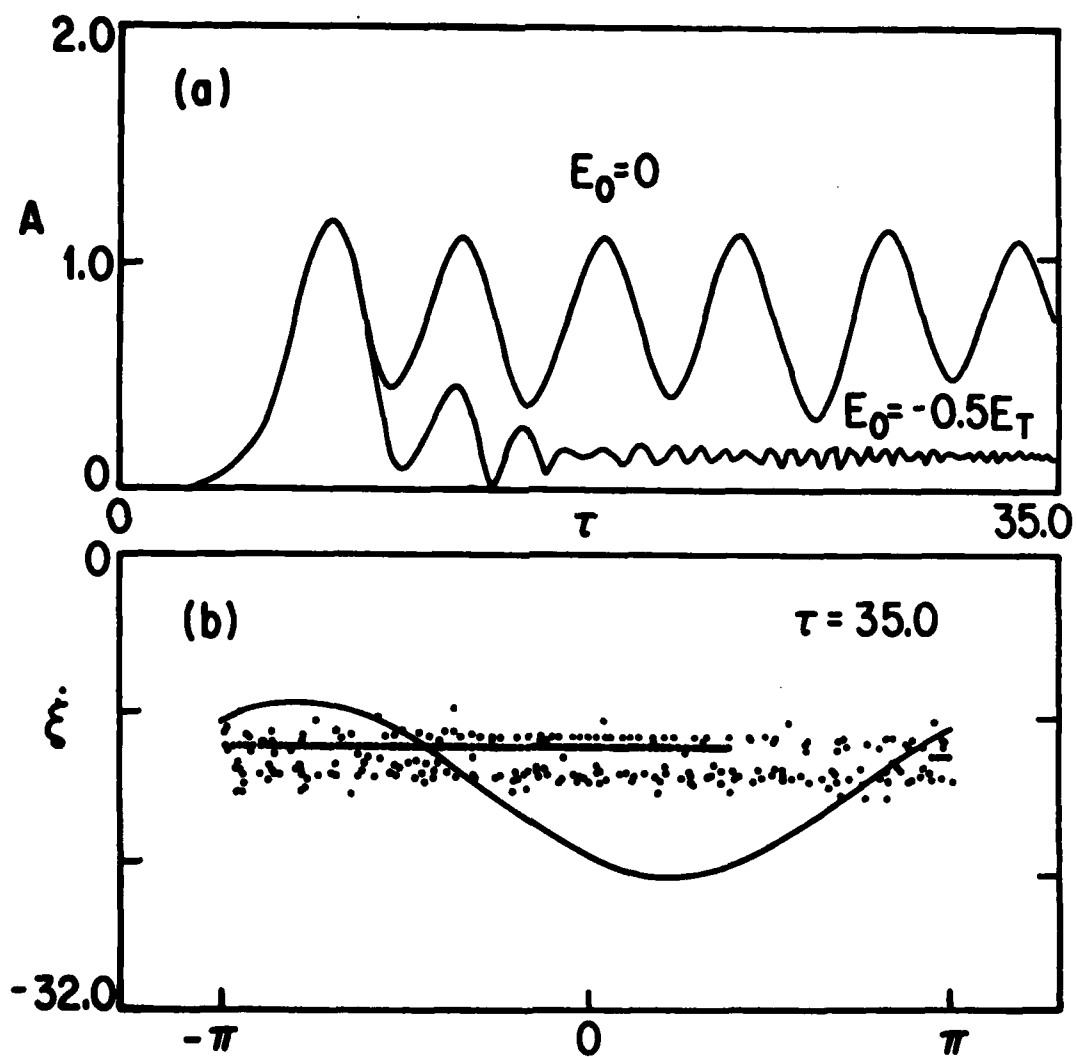


Fig. 5

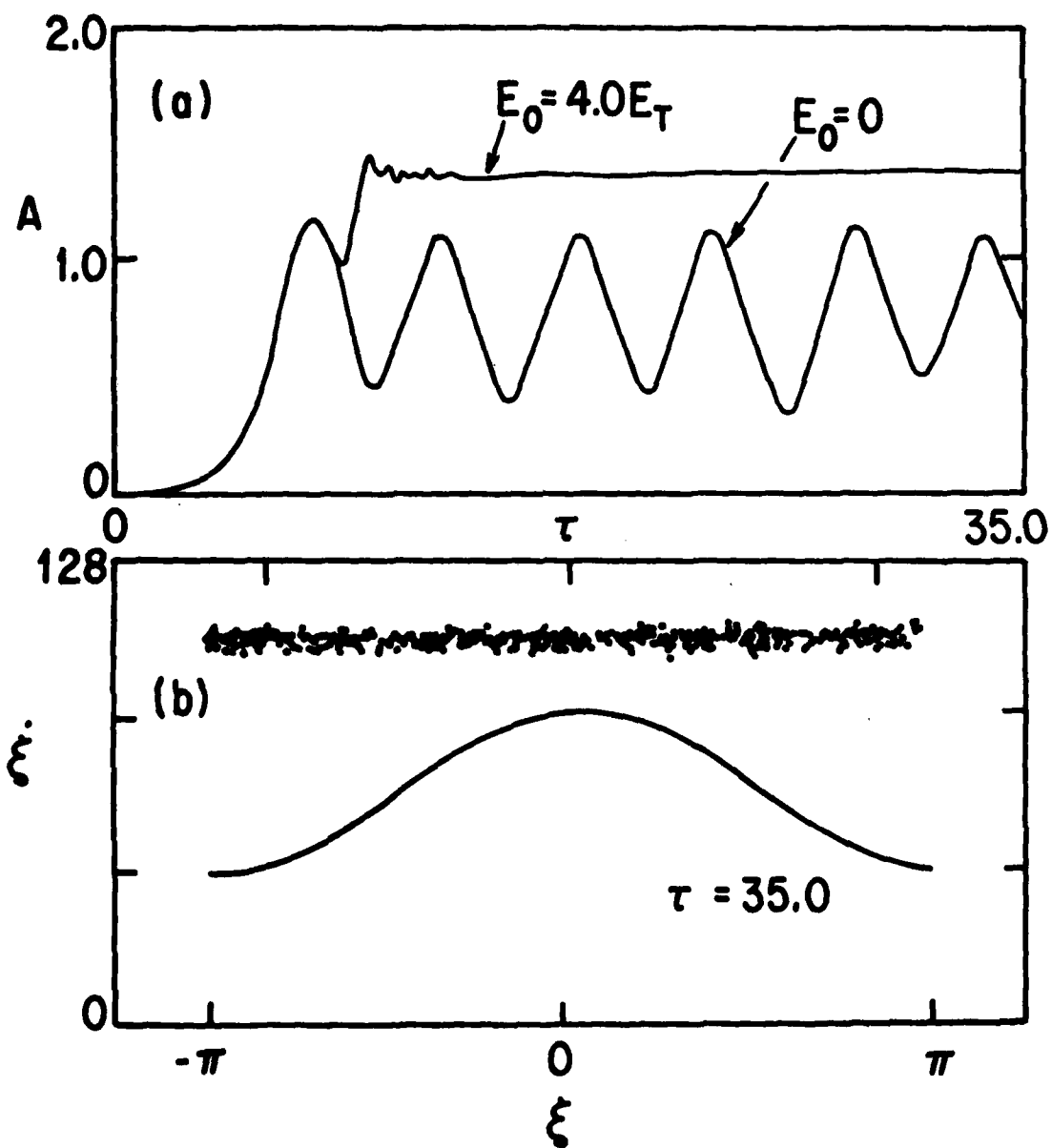


Fig. 6

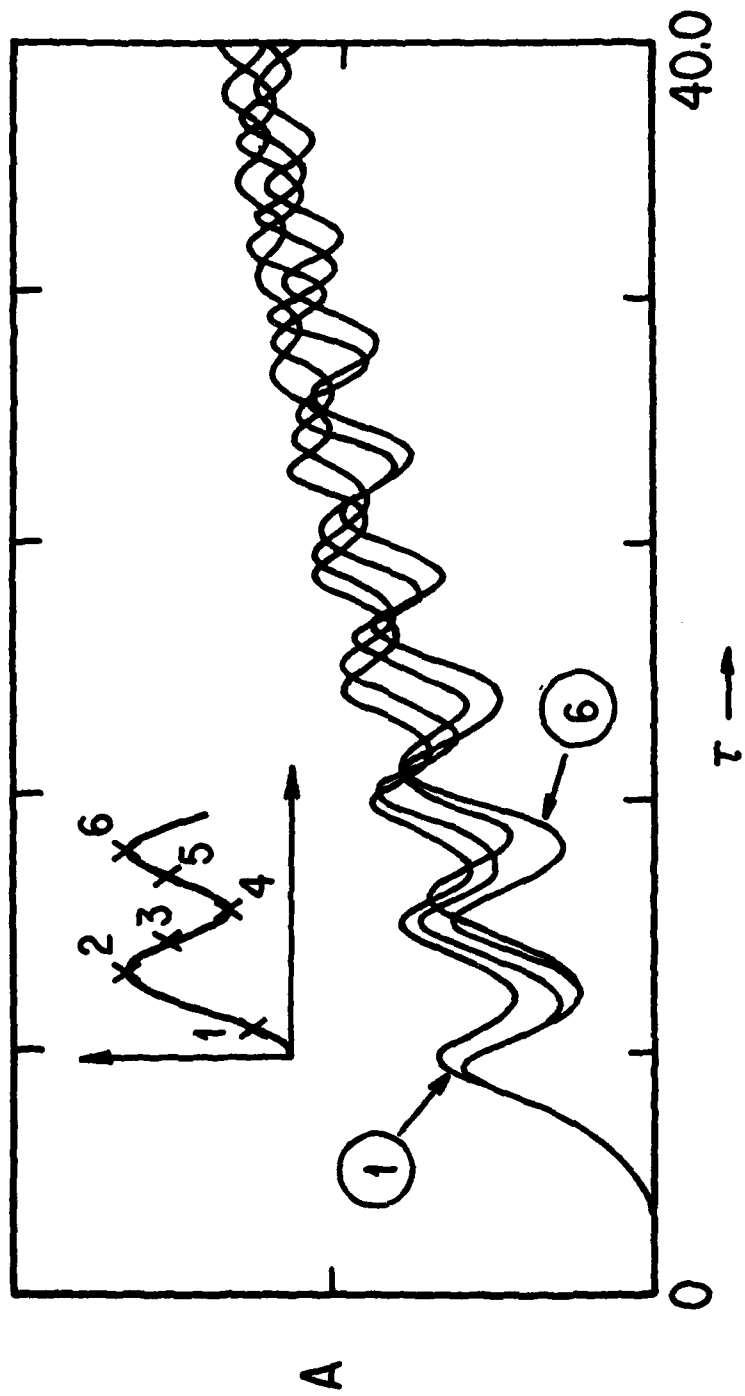


FIG. 7

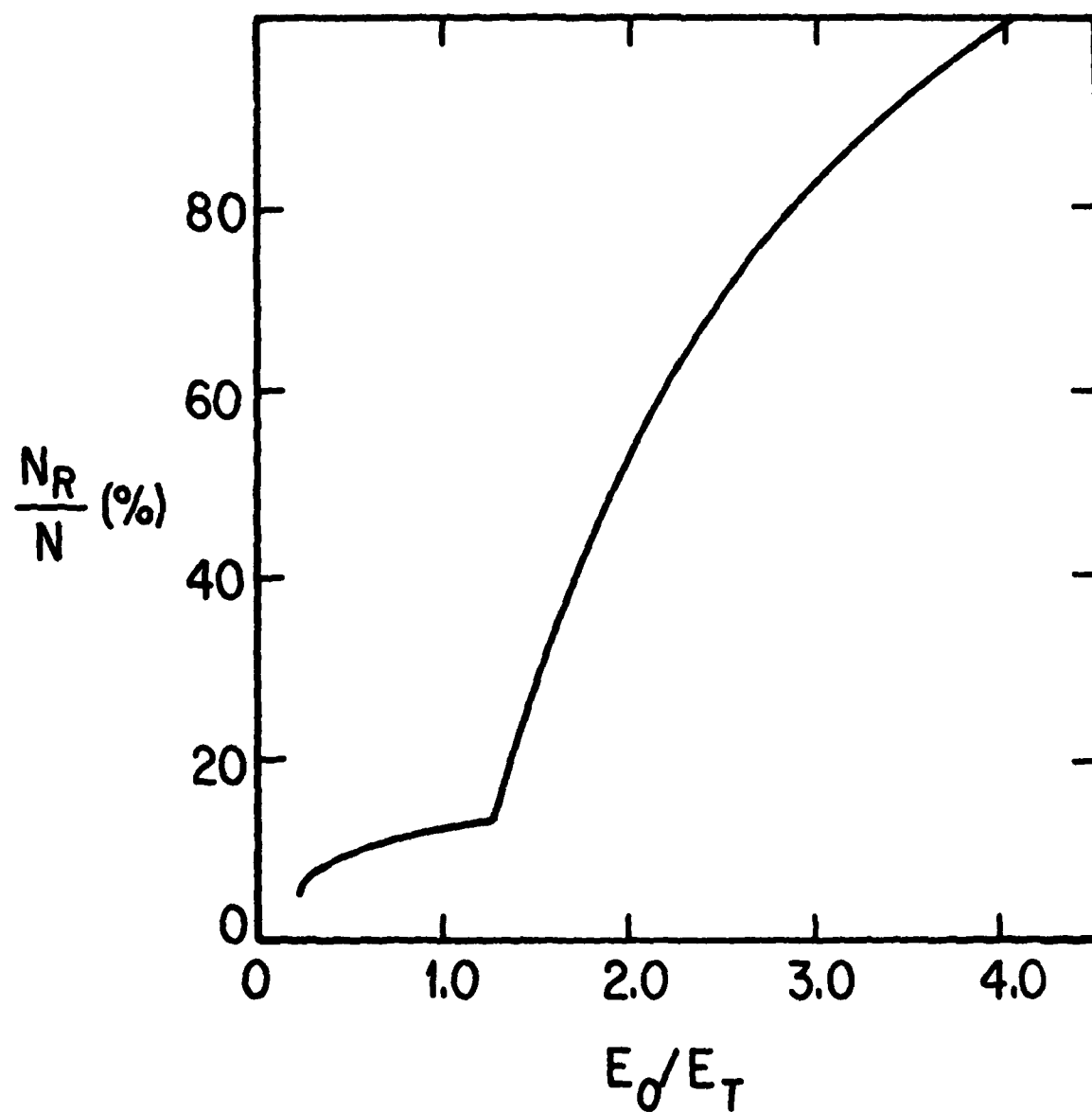


Fig. 8

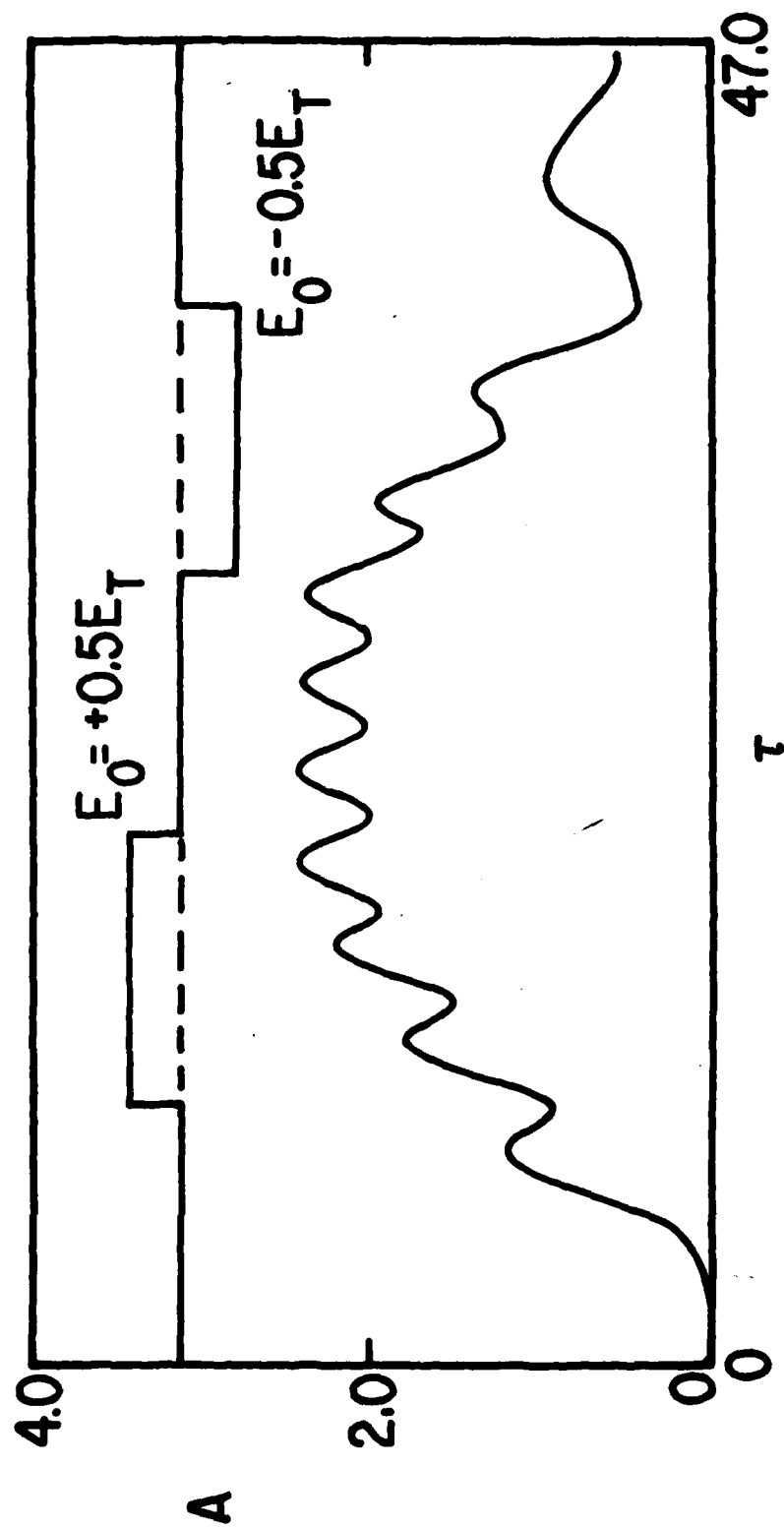


Fig. 9

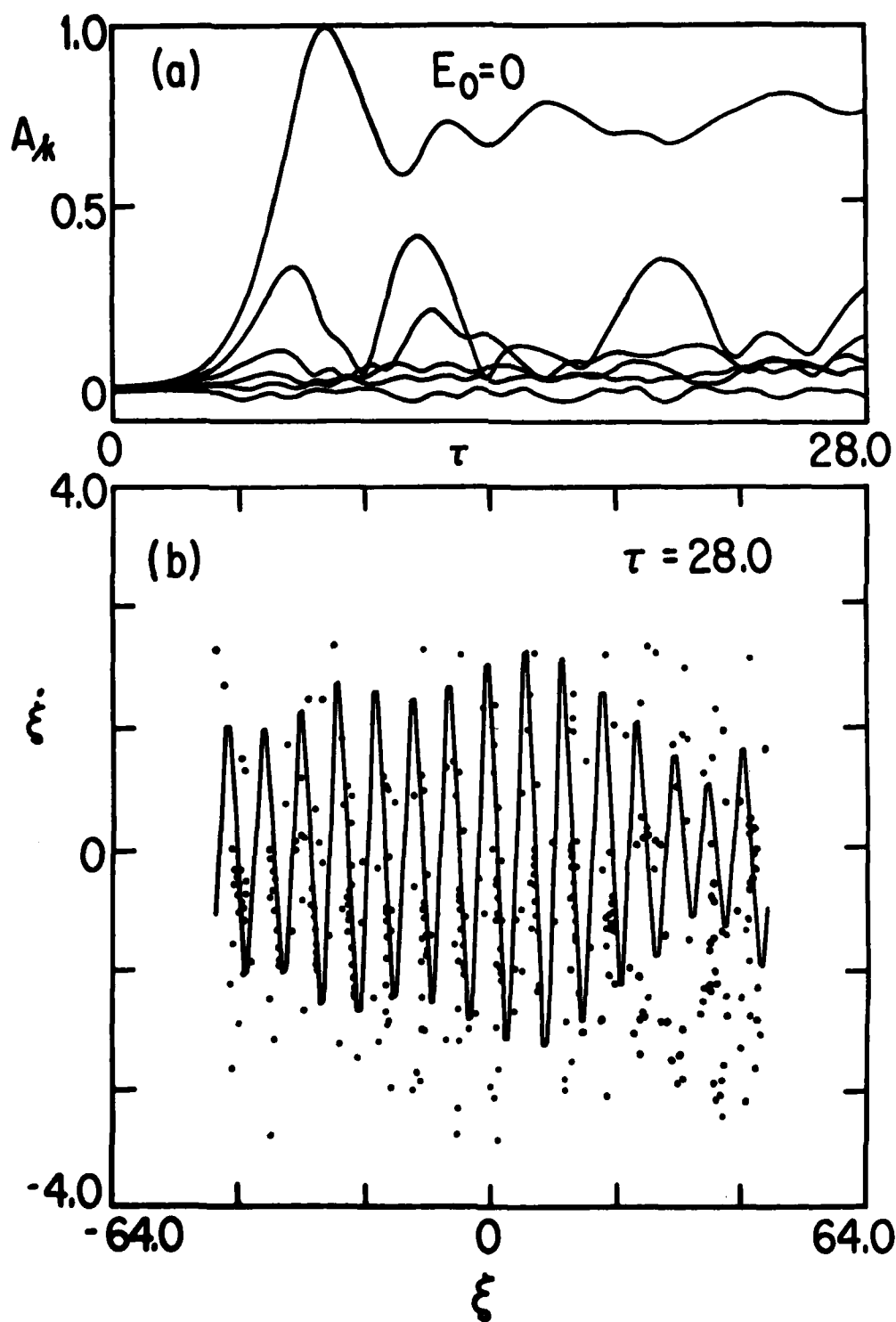


Fig. 10

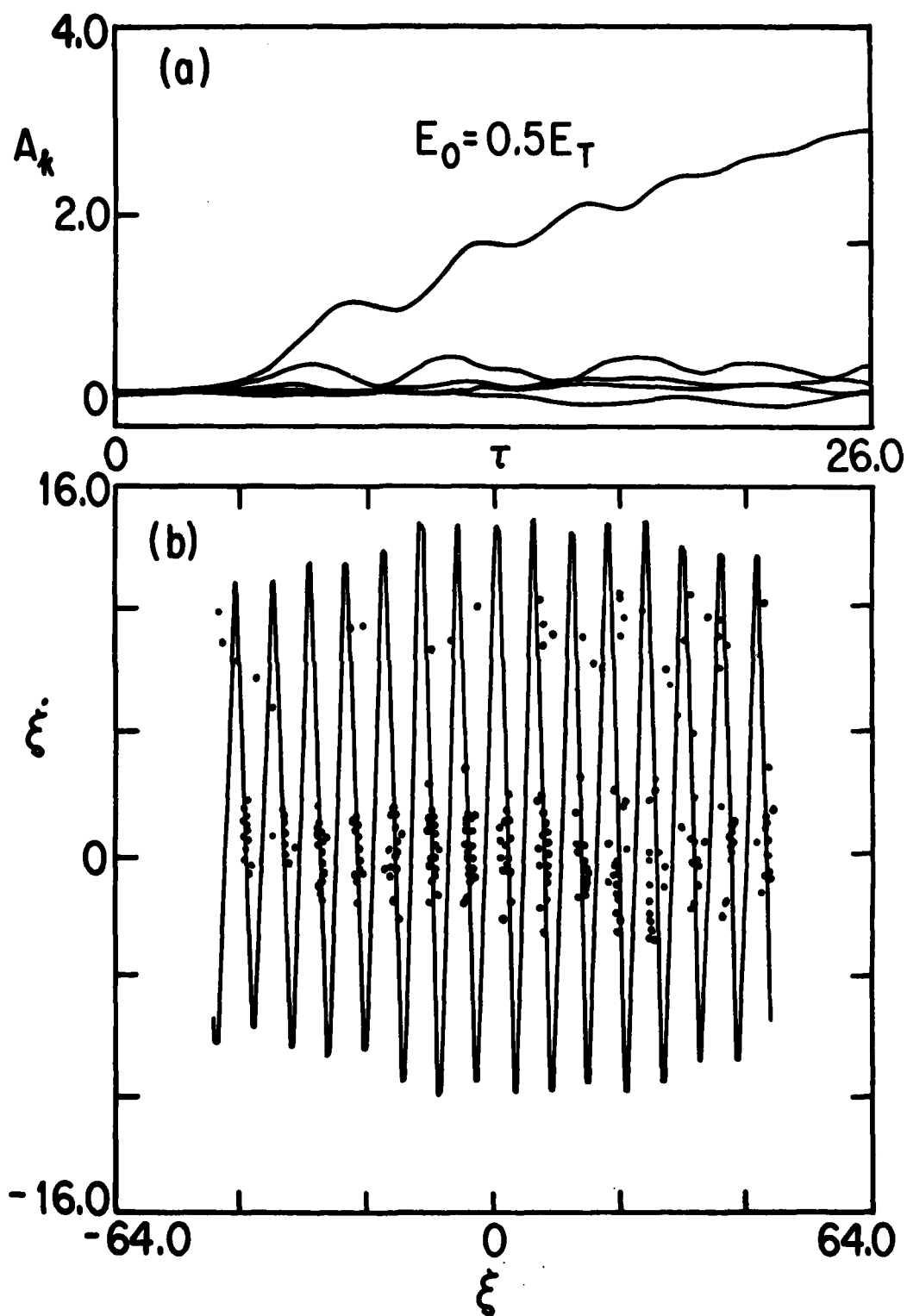


Fig. 11

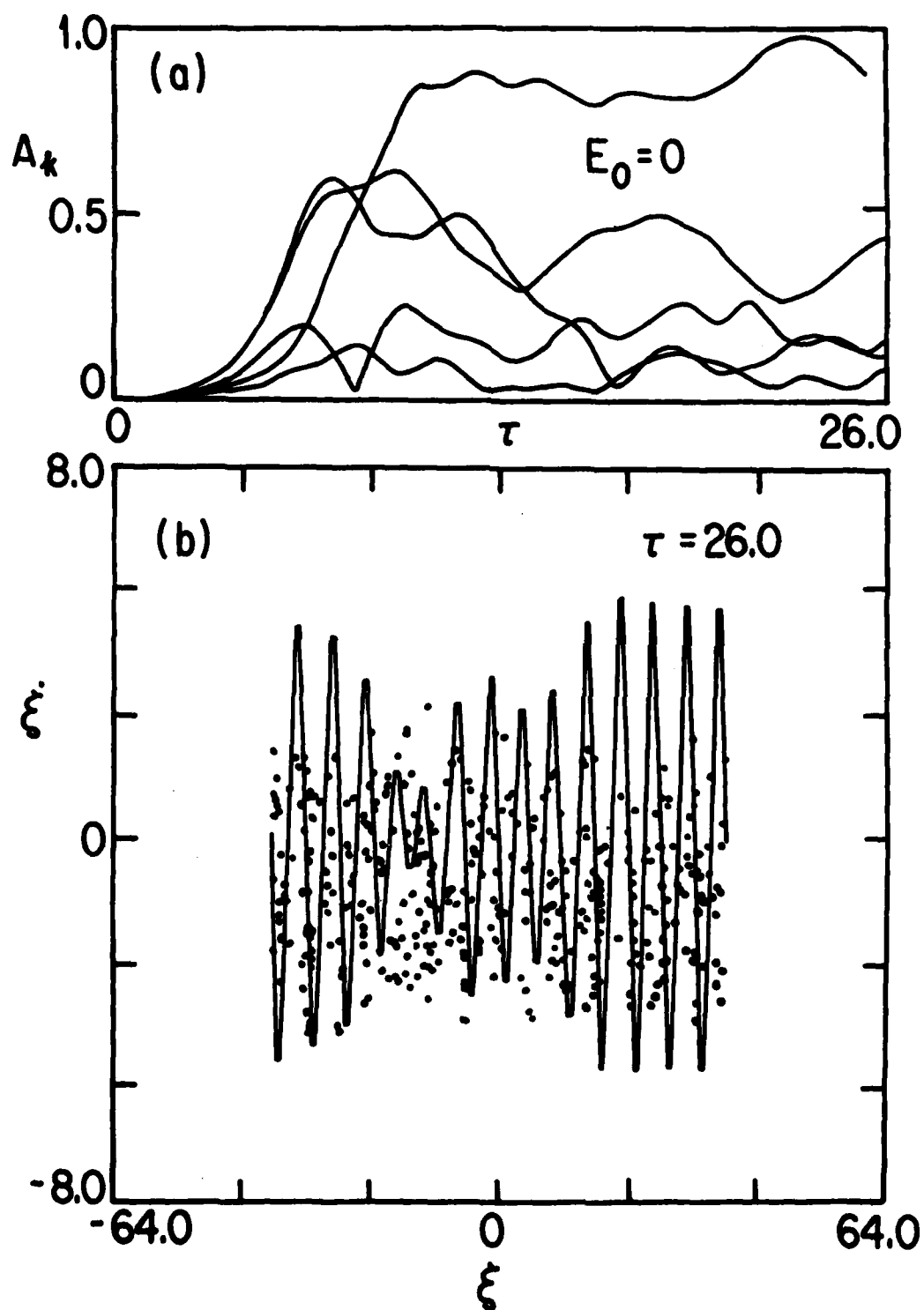


Fig. 12

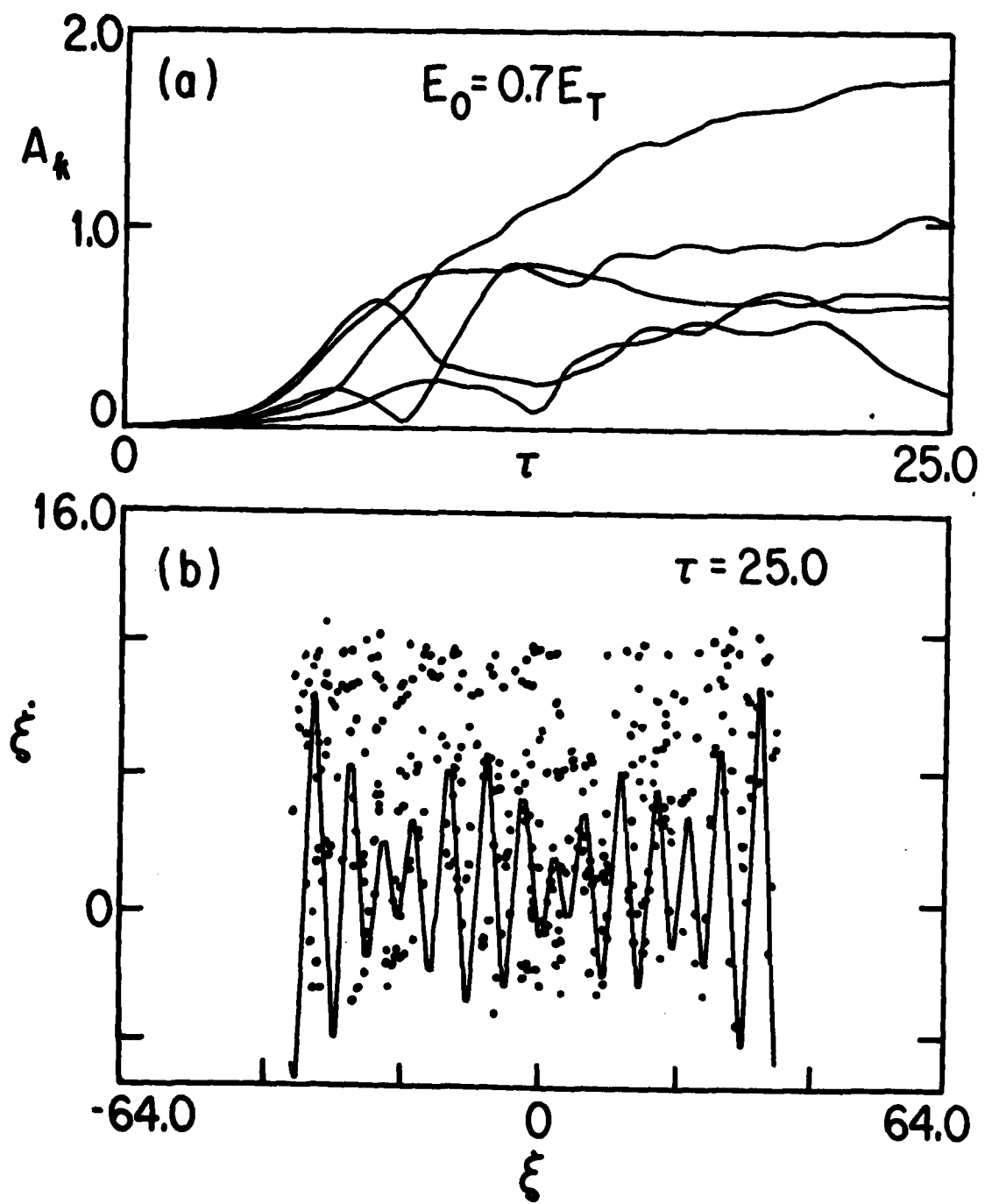


Fig. 13

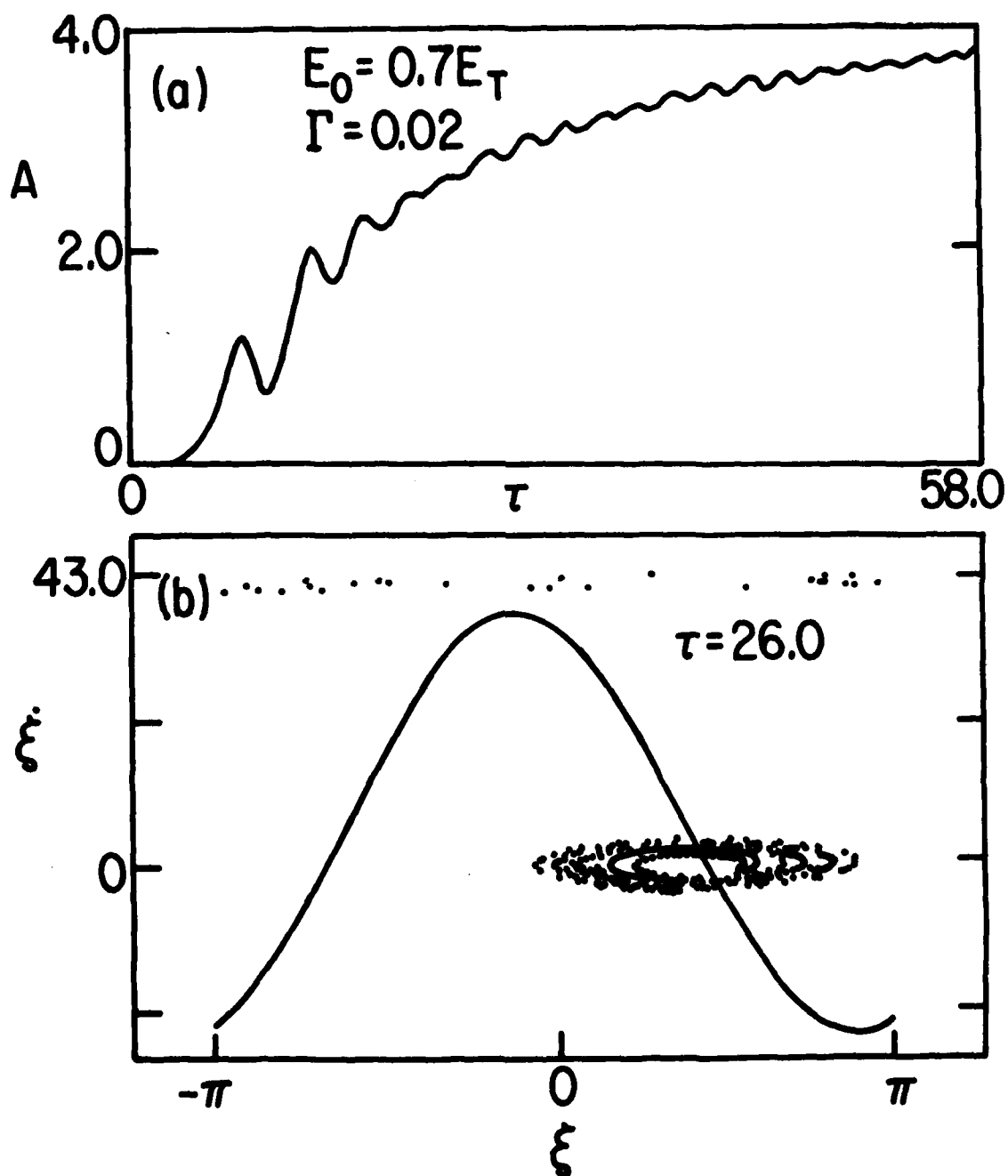


Fig. 14

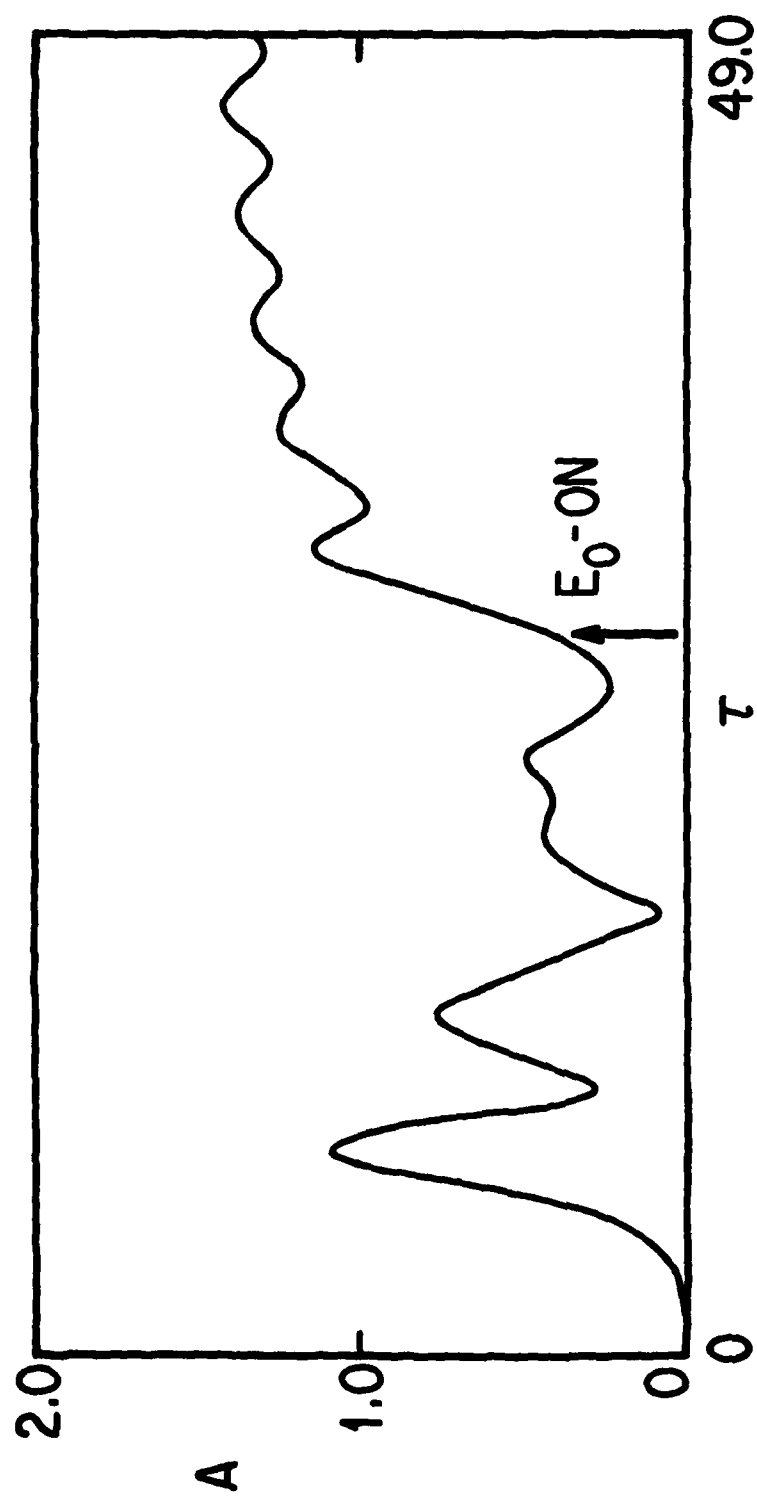


Fig. 15

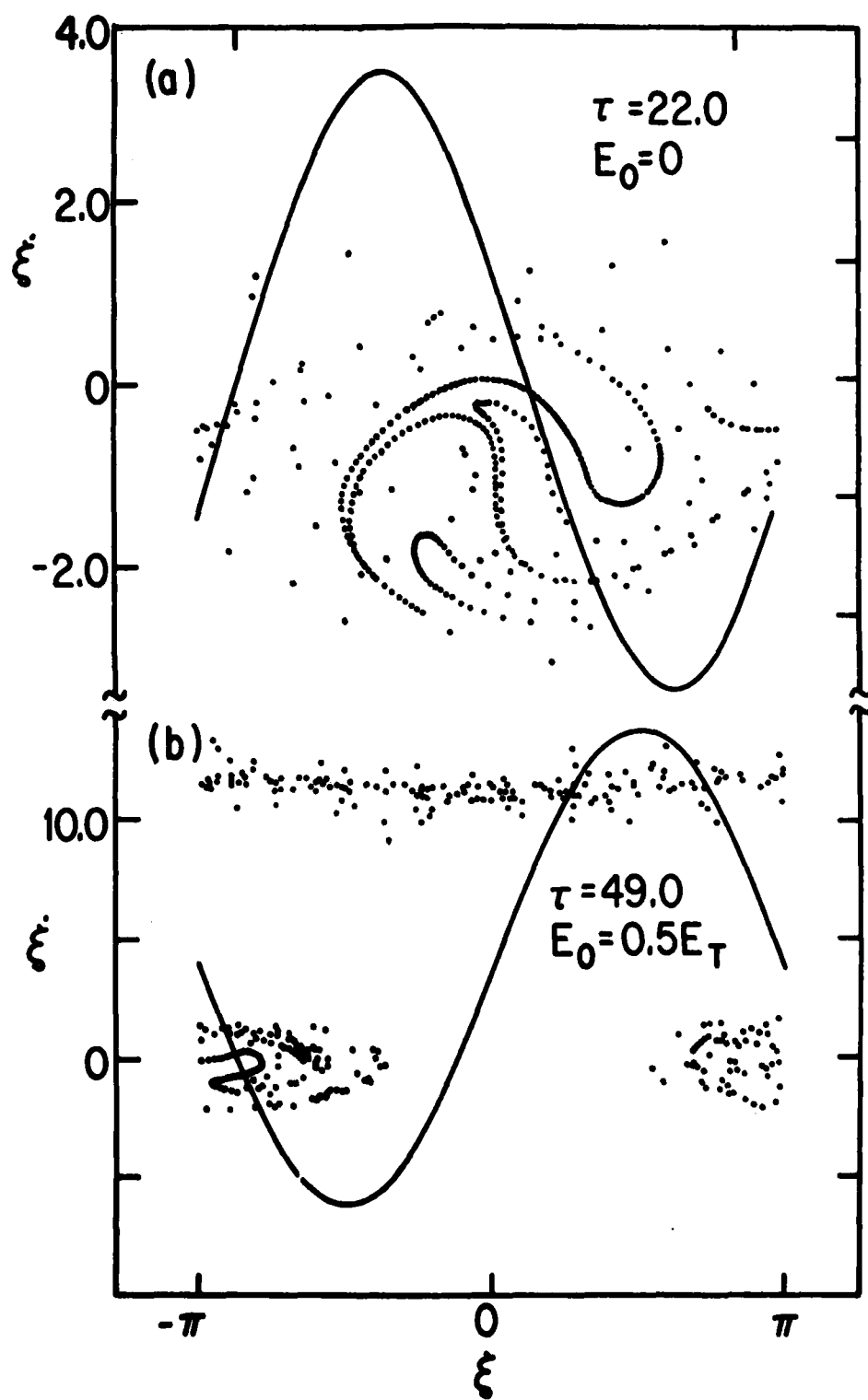


Fig. 16

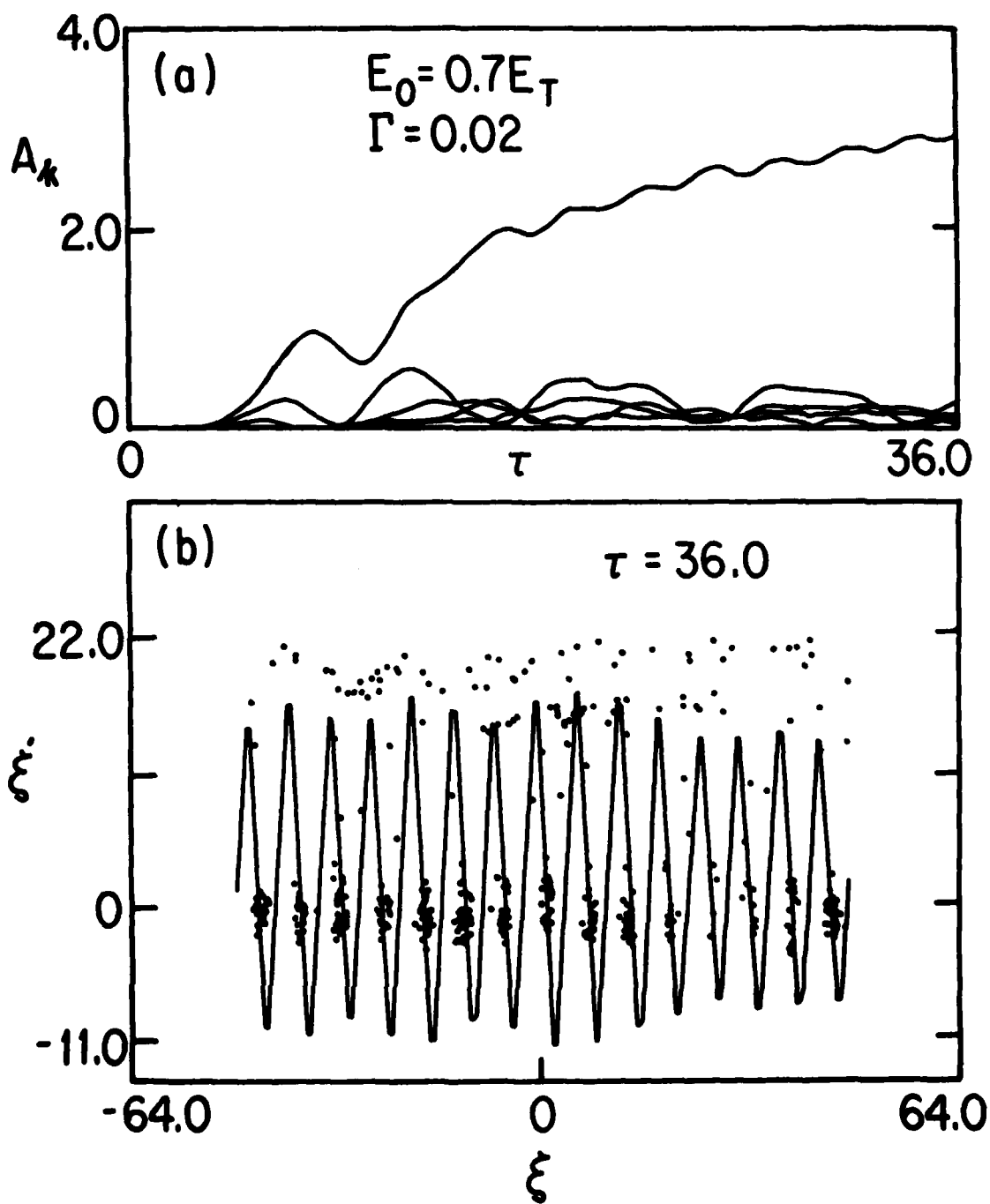


Fig. 17

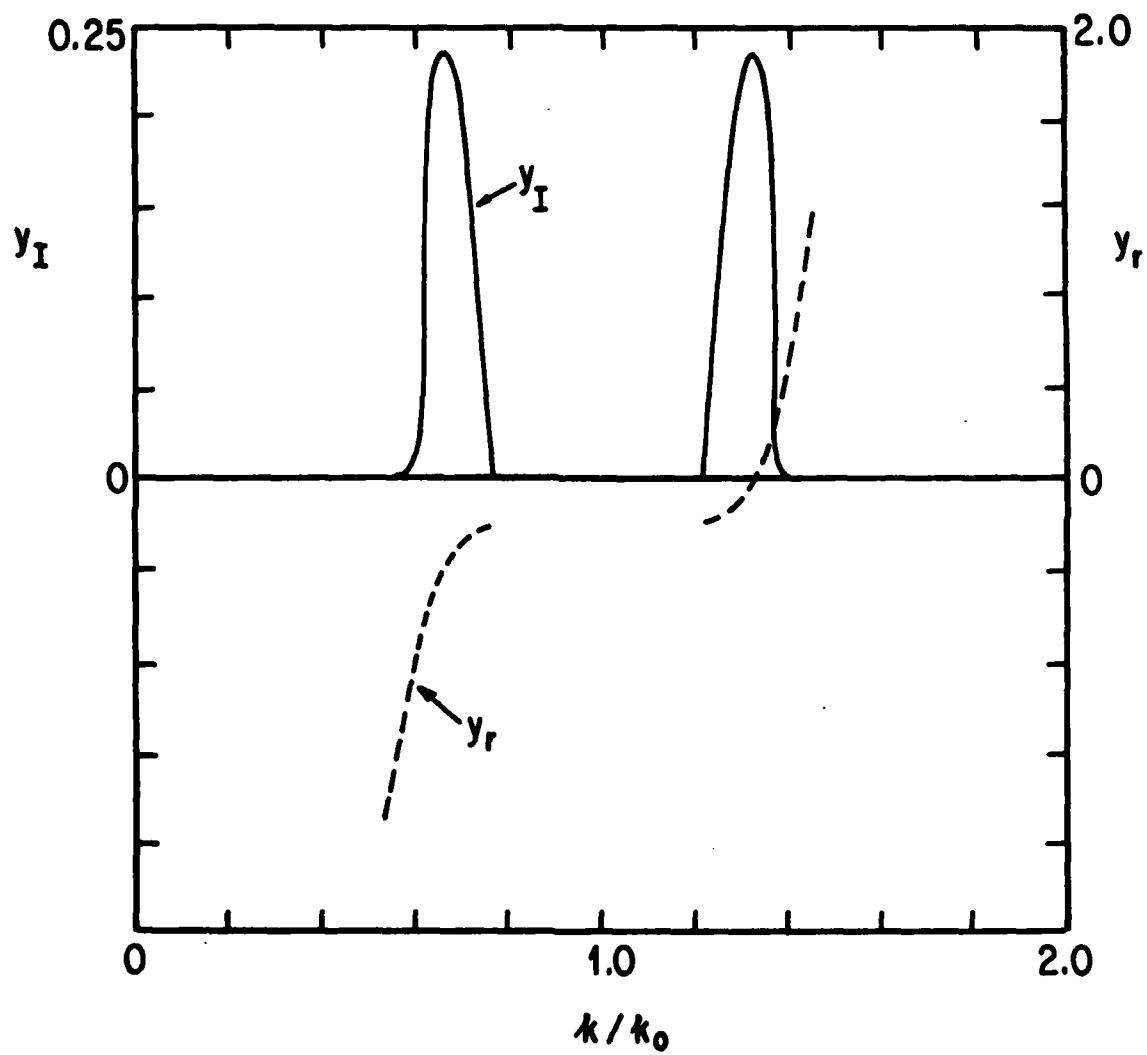


Fig. 18

- PPG-382 "Stimulated Brillouin Scattering and Backscatter of CO₂ Laser Radiation From a Laser-Altered Arc Plasma",
Mort J. Herbst, dissertation, January (1979).
- PPG-383 "Small-Scale Magnetic Fluctuations Inside the Macrotron Tokamak", S. J. Zweben, C. R. Menyuk, and R. J. Taylor.
Submitted to Phys. Rev. Lett., January (1979).
- PPG-384 "A High Efficiency Free Electron Laser", A. T. Lin and J. M. Dawson. Submitted to Phys. Rev. Lett., January (1979).
- PPG-385 "A Parametric Study of Electron Multiharmonic Instabilities in the Magnetosphere", M. Ashour-Abdalla, C. F. Kennel
and M. Livesey. Submitted to J. of Geophys. Res., January (1979).
- PPG-386 "Global Formalism for Ballooning-Type Modes in Tokamaks", Y. C. Lee and J. M. Vandam, submitted to Phys. Rev.
Lett., October (1978).
- PPG-387 "On the Origin of Plasmaspheric Hiss: the Importance of Wave Propagation and the Plasma-Pause", R. M. Thorne,
S. R. Church, and D. J. Gorney, submitted to Geophys. Res., January (1979).
- PPG-388 "The New Alchemy Again -- Again", F. Chen, accepted by The Sciences, January (1979).
- PPG-389 "Stability of Drift-Wave Eigenmodes with Arbitrary Radial Wavelengths", Y. C. Lee, Liu Chen and W. M. Nevins,
submitted to Phys. Rev. Lett., February (1979).
- PPG-390 "Alternate Concepts in Magnetic Fusion", Frank Chen, to be published in Phys. Today, February (1979).
- PPG-391 "Enhanced Interaction between Electrons and Large Amplitude Plasma Waves by a DC Electric Field", J. N. Leboeuf
and T. Tajima, accepted by Phys. Fluids, February, (1979).
- PPG-392 "Coalescence of Magnetic Islands", P. L. Pritchett and C. C. Wu, submitted to Physics of Fluids, February (1979).
- PPG-393 "Formation of Double Layers", P. Leung, A. Y. Wong and B. H. Quon. Submitted to Phys. Fluids, February (1979).
- PPG-394 "Experiments on Magnetic Field Line Reconnection", R. L. Stenzel and W. Gekelman, submitted to Phys. Rev. Lett.,
February (1979).
- PPG-395 "Magnetospheric Multiharmonic Instabilities", Maha Ashour-Abdalla, C. F. Kennel, and D. D. Sentman, to be
published in the Proc. of the Symposium on Wave Instabilities in Space Plasmas, February (1979).
- PPG-396 "Comment on the Ballooning Criterion for Multipoles", E. A. Adler and Y. C. Lee, to be submitted to
Phys. Fluids, February (1979).
- PPG-397 "Laser Electron Accelerator", T. Tajima and J. M. Dawson, submitted to Phys. Rev. Lett., March (1979).
- PPG-398 "Pulsar Magnetospheres", C. F. Kennel, F. S. Fujimura, and R. Pellat, to be published in the Proceedings of
NASA/JPL workshop on Planetary and Astrophysical Magnetospheres, a special edition of Space Science Reviews,
March (1979).
- PPG-399 "Nuclear Power as an Ultimate Power Source", F. Chen, March (1979).
- PPG-400 "Experimental Observations of Highly Nonlinear States in Plasmas", A. Y. Wong, April (1979).
- PPG-401 "The Onset of Stochasticity in a Superadiabatic Mirror," by C. R. Menyuk and Y. C. Lee, April (1979) submitted to
Phys. Rev. Lett. and Phys. Fluids.
- PPG-402 "Linear Stability of High-m Drift-Tearing Modes", D. A. D'Ippolito, Y. C. Lee, and J. F. Drake, March (1979)
submitted to Phys. Fluids.
- PPG-403 "Aspects of Pulsar Evolution", F. S. Fujimura and C. F. Kennel, March (1979) submitted to Astrophysical Journal.
- PPG-404 "A Magnetohydrodynamic Particle Code with Force Free Electrons for Fluid Simulations", T. Tajima, J. N. Leboeuf,
and J. M. Dawson, April (1979) submitted to Journal of Computational Physics.
- PPG-405 "The Kelvin-Helmholtz Instability in Supersonic and Superalvenic Fluids", by T. Tajima and J. N. Leboeuf,
April (1979), submitted to Phys. Fluids.
- PPG-406 "RF-Heating of Toroidal Plasmas", E. Canobbio, April (1979), Topics in Applied Physics (Springer-Verlag):
Controlled Thermonuclear Fusion - Magnetic Confinement.
- PPG-407 "Cross-Field Electron Transport Due to Thermal Electromagnetic Fluctuations", A. T. Lin, J. M. Dawson, and H. Okamoto,
April (1979), submitted to Phys. Rev. Lett.
- PPG-408 "Magnetospheric Reconnection, Substorms, and Energetic Particle Acceleration", F. V. Coroniti and C. F. Kennel, May (1979)
To be published in the Proceedings of the La Jolla Workshop on Particle Acceleration Processes in Space and
Astrophysics, American Institute of Physics, 1979.

- PPG-409 "Confinement of Plasmas by Surface Magnetic Fields (THE SURMAC CONCEPT)", Alfred Y. Wong, May (1979).
- PPG-410 "Electron Distribution Functions Associated with Electrostatic Emissions in the Dayside Magnetosphere", D. D. Sentman, L. A. Frank, C. F. Kennel, D. A. Gurnett and W. S. Kurth.
- PPG-411 "Simulation of Lower Hybrid Heating in a Nonuniform Plasma Slab", G. J. Morales, J. M. Dawson, and V. K. Decyk, May (1979), submitted to Phys. Fluids.
- PPG-412 "Let Us Become Familiar with the UCLA Simulation Codes", T. Tajima, May (1979).
- PPG-413 "Formation of Neutral Sheets and Slow Shocks in a Laboratory Experiment on Reconnection", W. Gekelman, R. L. Stenzel, May (1979), submitted to Jr. Geophys. Res.
- PPG-414 "Electrostatic and Induced Electric Fields in a Reconnection Experiment", R. L. Stenzel and W. Gekelman, May (1979) submitted to Jr. Geophys. Res.
- PPG-415 "Kinetic Theory of Ballooning Instabilities", James W. Van Dam, June (1979) Thesis.
- PPG-416 "Diffuse Jovian Aurora Modulated by Volcanic Activity on Io", R. M. Thorne and B. T. Tsurutani, June (1979) submitted to Geophys. Res. Lett.
- PPG-417 "Forced Tearing and Reconnection of Magnetic Fields in Plasmas", W. Gekelman and R. L. Stenzel, June (1979), submitted to Phys. Rev. Lett.
- PPG-418 "Radiation Protection in Tokamak Fusion Research", J. W. Horner and R. J. Taylor, June (1979).
- PPG-419 "Saturation and Reflectivity for the Brillouin Backscattering Instability", T. Tajima, July (1979).
- PPG-420 "Theory of Double Resonance Parametric Excitation in Plasmas II", B. D. Fried, A. Adler, and R. Bingham, July (1979), submitted to J. Plas. Phys.
- PPG-421 "Study of Low Frequency Microinstabilities in the Microtor Tokamak Using Far Infra Red Laser Scattering", A. Simion, A. Nase, W. A. Peebles and N. C. Luhmann, Jr., July (1979).
- PPG-422 "Observation of Stimulated Brillouin Scattering in a Microwave Plasma Interaction Experiment", H. E. Huey, A. Nase, and N. C. Luhmann, Jr., July (1979).
- PPG-423 "Saturation of Brillouin Back Scatter", M. J. Herbst, C. E. Clayton and F. F. Chen, July (1979), submitted to Phys. Rev. Lett.
- PPG-424 "Studies of Back Side Scatter and Back Scatter from Preionized Plasmas", M. J. Herbst, C. E. Clayton, W. A. Peebles, and F. F. Chen, August (1979), submitted to Phys. Fluids.
- PPG-425 "Equilibrium and Stability of High- β Toroidal Multipoles", D. A. D'Ippolito, E. A. Adler, and Y. C. Lee, July (1979), submitted to Phys. Fluids.

